3476–3495 *Nucleic Acids Research, 2020, Vol. 48, No. 7* *Published online 13 February 2020*
doi: 10.1093/nar/gkaa082

The Drosophila MLR COMPASS complex is essential for programming *cis*-regulatory information and maintaining epigenetic memory during development

Claudia B. Zraly[1], Abdul Zakkar[2], John Hertenstein Perez[1], Jeffrey Ng[1,2], Kevin P. White[3], Matthew Slattery[3,4] and Andrew K. Dingwall[1,5,*]

[1]Department of Cancer Biology, Stritch School of Medicine, Loyola University Chicago, Maywood, IL 60153, USA, [2]Department of Biology, Program in Bioinformatics, Loyola University Chicago, Chicago, IL 60660, USA, [3]Institute for Genomics and Systems Biology and Department of Human Genetics, University of Chicago, Chicago, IL 60637, USA, [4]Department of Biomedical Sciences, University of Minnesota Medical School, Duluth, MN 55812, USA and [5]Department of Pathology & Laboratory Medicine, Stritch School of Medicine, Loyola University Chicago, Maywood, IL 60153, USA

Received September 13, 2019; Revised January 17, 2020; Editorial Decision January 30, 2020; Accepted January 30, 2020

ABSTRACT

The MLR COMPASS complex monomethylates H3K4 that serves to epigenetically mark transcriptional enhancers to drive proper gene expression during animal development. Chromatin enrichment analyses of the Drosophila MLR complex reveals dynamic association with promoters and enhancers in embryos with late stage enrichments biased toward both active and poised enhancers. RNAi depletion of the Cmi (also known as Lpt) subunit that contains the chromatin binding PHD finger domains attenuates enhancer functions, but unexpectedly results in inappropriate enhancer activation during stages when hormone responsive enhancers are poised, revealing critical epigenetic roles involved in both the activation and repression of enhancers depending on developmental context. Cmi is necessary for robust H3K4 monomethylation and H3K27 acetylation that mark active enhancers, but not for the chromatin binding of Trr, the MLR methyltransferase. Our data reveal two likely major regulatory modes of MLR function, contributions to enhancer commissioning in early embryogenesis and bookmarking enhancers to enable rapid transcriptional re-activation at subsequent developmental stages.

INTRODUCTION

COMPASS complexes (Complex of Proteins Associated with Set1) catalyze the methylation of H3K4, considered a modification associated with transcription activation, with di- and trimethylation around active promoters and monomethylation at enhancers. Metazoans contain three related COMPASS complexes including two with specialized functions. MLX complexes (MLL1/4(2), TRX) maintain promoter nucleosome di- and trimethylation, while MLR complexes (MLL2(4)/MLL3, TRR) monomethylate enhancer nucleosomes (1,2).

Enhancers (also known as *cis*-regulatory modules, CRM) serve to coordinate transcription events at the cellular and organismal levels through gene regulatory networks that control both the timing and level of gene activity during animal development (3). Enhancers contain transcription factor binding sites and are controlled through the integration of multiple signal inputs including nucleosome remodeling, histone modification, RNA Polymerase II (RNAP II)-dependent transcription and association of factors to facilitate direct enhancer-promoter contacts (4–7). The most consistent genomic feature of enhancers is monomethylated H3K4 (H3K4me1), with different combinations of histone marks and histone variants associated with either active, poised or primed enhancers (5,8–10). While H3K4me1 serves to mark all enhancers (11,12), monomethylation alone is insufficient, as activation requires acetylation of H3K27 mediated by the CBP/p300 histone acetyltransferase, while poised enhancers are marked by H3K27me3

*To whom correspondence should be addressed. Tel: +1 708 327 3141; Email: adingwall@luc.edu
Present addresses:
John Hertenstein Perez, Public Health Institute of Metropolitan Chicago, IL, USA.
Abdul Zakkar, University of Illinois College of Medicine, Chicago, IL, USA.
Kevin P. White, Tempus Inc., Chicago, IL, USA.
Jeffrey Ng, Department of Genetics, Washington University in St. Louis, School of Medicine, St. Louis, MO, USA.

catalyzed by the EZH2 methyltransferase (5). Removal of the H3K27 methyl groups by the UTX/KDM6A demethylase subunit of the MLR complex allows for acetylation and activation (13).

The MLR complexes are important for proper enhancer regulation, including the pioneering and priming of enhancers *de novo*, as well as modulating enhancer activity and functions important for the correct timing of enhancer utilization and communication with promoters (11–16). MLR complexes are recruited to enhancers by transcription factors to activate target genes during cellular differentiation (17). In murine embryonic stem cells (ESC), Mll2(4)/Kmt2d is required for cellular differentiation and reprogramming to a pluripotent state, but not ESC maintenance (18). Further, both Mll3/Kmt2c and Mll2(4)/Kmt2d as well as H3K4me1 are important for promoting or stabilizing enhancer/promoter interactions in ESCs through the recruitment of cohesin complexes (16). Similarly, Drosophila Trr methyltransferase activity and cohesin are important for precise enhancer control during development (12). While the functions of the SET domain methyltransferase activity of the KMT2C/D and Trr MLR proteins in transcription regulation have been explored, less is understood regarding the role of the highly conserved PHD finger clusters that participate in heterotypic protein interactions and histone binding (19–21). A split of these two features into separate proteins during evolution in the schizophora dipterans, including Drosophila, has allowed for an examination of the unique contribution of the PHD domains in regulating MLR complex functions in a developmental context (20,22,23). Drosophila Cmi contains the two PHD finger clusters, a high mobility group (HMG) domain and nuclear receptor interaction motifs found in the N-terminal portion of KMT2C/D. Cmi is essential for viability and required for MLR complex functions, including interactions with transcription factors, such as the hormone regulated ecdysone receptor (EcR), recognition and binding to histones, and proper tissue patterning (20,22). Null mutations in *cmi* result in L2 stage larval lethality, while tissue-specific shRNAi depletion leads to wing vein and eye defects (20,22). The Drosophila MLR (Cmi-Trr) complex directly participates in regulating multiple developmental signaling pathways, including Tgfβ/Dpp, Notch and Hippo (22,24–26), though the specific gene targets are not well defined.

The MLR complexes are essential for viability, tissue-specific transcription regulation, cellular differentiation and genome reprogramming (15,18,22,27,28). In vertebrate animals, MLR subunit mutations have been linked to developmental disorders, metabolic dysregulation and a large variety of cancers, (1,29–36). An inability to properly orchestrate essential gene regulatory events during embryogenesis underlies many developmental defects (1). Reduced germline functions of human MLL2(4)/KMT2D and UTX/KDM6A are associated with Kabuki syndrome, while loss of MLL3/KMT2C is linked to Kleefstra syndrome, both characterized by skeletal abnormalities and intellectual disorders (37–39). Similarly, loss or gain of function alterations of Drosophila Cmi or Trr result in significant tissue patterning and growth defects, immune dysregulation, cell death and altered metabolic signaling (12,20,22,24). Further, somatic loss or reduced functions of KMT2C and KMT2D are among the most frequent alterations in many cancers (1,31,40).

At present, there is no comprehensive view of MLR complex functions during normal animal development. We first characterized the genomic enrichments of Cmi over multiple developmental stages and observed dynamic localization at both enhancers and promoters. Genetic depletion of Cmi resulted in both decreased transcription as well as derepression of certain gene enhancers depending on developmental stage, suggesting a possible unanticipated role for the complex in stabilizing poised or inactive enhancers. Importantly, Cmi subunit loss allows for Trr to be retained on chromatin, but impairs both H3K4me1 and H3K27ac, implicating the PHD finger portion of the MLR proteins as essential for the proper marking and activation of enhancers and maintaining enhancer genomic features during development.

MATERIALS AND METHODS

Drosophila culture

Drosophila Schneider (S2) cells were cultured in Schneider's medium supplemented with 10% FBS at 25°C. Hormone induction was achieved by addition of 20-hydroxyecdysone (20-HE; Sigma) to a final concentration of 1 μM for 6 or 24 h (41). Knockdown of *cmi, trr* and *Nipped B* in cultured S2 cells was performed using RNAi. Double-stranded RNA was prepared using gene-specific primers (Supplementary Table S1) with added T7 polymerase priming sites and the MEGAscript kit (ThermoFisher) according to manufacturer's protocols. dsRNA was added to cultured S2 cells and incubated for 5 days prior to assay or addition of 20-HE for 6 h. Knockdown efficiency was assessed by quantitative RT-PCR (Supplementary Figure S1) and western blot using specific antibodies (20).

Drosophila crosses were performed at either 25°C or 29°C with flies grown on standard yeast/dextrose/cornmeal food. shRNAi knockdowns (Supplementary Figure S1) were performed by crossing a UAS_{Gal4} driver line to the appropriate inverted repeat (IR)-containing line and scoring the progeny (20). Drosophila stocks containing Gal4 drivers, gene mutations or inverted repeats were as described or obtained from the Bloomington Drosophila Stock Center: *cmi-IR* (20), *trr-IR* (20), *NippedB-IR* (#36614, #32406), *UAS-Grh* (#42227), *grh-IR* (chr3) (#42611), *grh-IR* (chr2) (#36890), *UAS-HA-Cmi* (20), *NippedB[02047]* (#11143), *NippedB[NC138]* (#7163), *GawB69B-Gal4* (#1774), *C765-Gal4* (#36523), *Sgs3-Gal4* (#6870), *en-Gal4(e16E)* (#30564), *Kdm5-IR* (chr2) (#36652), *Kdm5-IR* (chr3) (#28944), *UAS-Kdm5* (42) from J. Secombe.

RNA extraction, RT-qPCR and RNA-sequencing

Staged animals of the appropriate genotypes were collected and total RNA was prepared, DNase digested and reverse transcribed, as previously described (22). Animals were staged according to standard guidelines using morphological landmarks (43,44) and included the use of 0.05%

bromophenol blue as a dye marker in the Drosophila growth medium to distinguish blue verses clear gut third instar larvae. Transcript levels were analyzed by SYBR Green quantitative real time PCR on reverse transcriptase reactions (qRT-PCR) performed in triplicate using PowerUp SYBR Green Master mix on a QuantStudio 6 Flex Real time PCR machine (Applied Biosytems). Levels of mRNA were normalized to the expression of the ribosomal gene *RpL32* and analyzed by the comparative $2^{-\Delta\Delta}C_t$ method. Primer sequences are provided in Supplementary Table S1.

RNA-sequencing experiments were performed on whole blue and clear gut third instar larvae of the genotypes: wild type control (*GawB69B-Gal4*), *GawB69B-Gal4>cmi-IR* and GawB69B-Gal4>trr-IR. Total RNA was prepared from pools of 20 BG and CG larvae of the appropriate genotype using the RNAqueous kit (Invitrogen). RNAs were DNAse digested (TURBO DNA-free, Invitrogen). The cDNAs were synthesized, adapters added, products amplified and sequenced by Beijing Genomics Institute (BGI) using an Illumina HiSeq 2000 (GEO accession GSE143239). After quality control, clean reads saved as FASTQ files were aligned to *Drosophila melanogaster* dm6 reference genome sequences with SOAPaligner/SOAP2 and validated using Bowtie. Transcripts were assembled with reads using Cufflink. Downstream analysis of gene expression included comparisons of differential expression of transcripts between knockdown animals and control as well as Gene Ontology (GO) and KEGG Pathway enrichment analysis. RNA sequencing files obtained from BGI or from GEO databases were interrogated for changes in gene expression and parsed into gene ontology groups. The RNA sequencing CSV files were filtered using Python script: [https://github.com/dingwall-lab/COMPASS-like/blob/master/filter.py]. Gene transcript differences associated with different genetic backgrounds at the same developmental stage with a P-value > 0.05 OR fold change < 1.3 were filtered out. The CSV file containing RNA expression data for the BG stage was filtered to include only increased expression compared to wild type, while the CSV file containing RNA expression data for the CG stage was filtered to include only decreased expression compared to wild type. The number of remaining genes in each file was counted in Excel (3442 genes in the BG stage, 1648 genes in the CG stage). These two sets of genes overlapped at 336 genes, as shown in the Venn Diagram in Figure 7B. The overlap gene set and Venn diagram were generated using Python script: [https://github.com/dingwall-lab/COMPASS-like/blob/master/count_like_terms.py; https://github.com/dingwall-lab/COMPASS-like/blob/master/venn_diagram.py].

Validation of the gene expression trends observed in the RNA-seq data was confirmed by RT-qPCR of individual genes (Supplementary Figure S2). Three genes displaying increased expression and three showing decreased expression relative to control animals in the RNA-seq datasets obtained for the *cmi-IR* BG larvae were chosen at random for subsequent quantification by RT-qPCR with the RNA samples used for the RNA sequencing and normalized to the expression of a ribosomal gene *RpL32*. In all cases, the trends were verified.

Gene ontology analyses. The RNA sequencing CSV files were filtered using Python script: [https://github.com/dingwall-lab/COMPASS-like/blob/master/filter.py]. Genes were filtered for P-value < 0.05, fold change > 1.3, and RPKM > 5. The CSV file containing RNA expression data for the BG stage was filtered to include only increased expression compared to wild type, while the CSV file containing RNA expression data for the CG stage was filtered to include only decreased expression compared to wild type. The remaining genes from these two files were then entered separately into the Database for Annotation, Visualization and Integrated Discovery (DAVID) v6.8 at [https://david.ncifcrf.gov/]. The functional annotation tool was used by entering the gene list, selecting the 'FLYBASE_GENE_ID' identifier, then selecting the 'Gene List' list type, then submitting. On the 'Annotation Summary Results' page, the 'Gene Ontology' dropdown is selected, then 'GOTERM_BP_DIRECT' is charted.

Chromatin immunoprecipitation

For S2 cells, after RNAi treatment and hormone (ecdysone) incubation when indicated, bulk chromatin was isolated using the Chromatin Immunoprecipitation (ChIP) Assay kit according to standard manufacturers protocols (Millipore Sigma). For whole animals, larvae of the appropriate genotype were collected and bulk chromatin was prepared according to the methods described in (45). Triplicates from at least three independent biological replicates were analyzed using the $2^{-\Delta\Delta}C_t$ method. Data is expressed as fold enrichment relative to input sample or percentage of input chromatin. IgG was used as a negative control. Primers used for ChIP-qPCR are provided in Supplementary Table S1.

Primary antibodies

Rabbit and guinea pig anti-Cmi/Lpt polyclonal sera (Pocono Rabbit Farm) were raised against amino acids residues 647–1069 fused to GST. The induced protein was purified on a glutathione agarose column (Sigma) and used for antibody production. Rabbit αSnr1 antibody was prepared as described (46). Mouse monoclonal antibody αRNA Polymerase II 8W (MMS-126R) was from Covance. Rabbit αH3 antibody (ab1791), αIgG (ab27478) and αHA (ab9110) were from Abcam. Rabbit αH3K27ac (39 133), αH3K27me3 (39 155), αH3K4me1 (39297) and αH3K4me3 (39 915) were from Active Motif. Lamin antibody (ADL40) was obtained from the Developmental Studies Hybridoma bank at the University of Iowa. Rabbit αTrr and rabbit αCBP antibodies were from A. Mazo (47). Rabbit αUtx antibody was a gift from A. Shilatifard (48,49). Guinea pig αCBP antibody was a gift from P. Harte (50). Rabbit αGrh (grainyhead) antibody was a gift from M. Harrison (51) and guinea-pig αGrh antibody was a gift from W. McGinnis.

Co-Immunoprecipitation

Soluble nuclear extracts were prepared from embryos expressing a hemagglutinin (HA) epitope tagged full length *cmi* transgene under UAS_{Gal4} control (20) according to the methods described in (52). Duplicate immunoprecipitations

were set up containing 80μg of soluble nuclear protein precleared with protein G-Sepharose beads (GE Healthcare) and incubated either with rabbit anti-HA or anti-IgG antibodies (Abcam) overnight. Protein complexes were then precipitated with protein-G Sepharose beads, washed extensively, then bound proteins were fractionated on SDS-PAGE gels and analyzed by western blotting. Input lanes represent 20% of starting material.

Preparation of Drosophila embryo and larval histone extracts

For histone isolation, soluble nuclear protein extracts were first prepared from fly embryos or staged third instar larvae. Histones were then acid extracted from soluble nuclear pellets by resuspension in 0.2N HCl overnight at 4°C with rotation. Samples were centrifuged for 5 min at 13 000 × g to remove debris. The acid soluble supernatants were saved and concentrated with 5× volume of acetone overnight at −20°C. Samples were centrifuged for 15 min at 13 000 × g and histone pellets were resuspended in sample buffer for Western analysis. Antibody to histone H3 was used to control for histone loading.

Imaginal Disc and polytene chromosome immunofluorescence staining

Expression of the UAS_{Gal4}: *cmi-IR* transgene was controlled by the *engrailed –Gal4* driver (*en-Gal4*) with crosses performed at 29°C. Dissected wing imaginal discs from wandering third instar larvae were fixed in 4% formaldehyde according to standard protocols as previously described (53). Wing discs were co-immunostained with rabbit αH3K4me1 (39297, Active Motif) antibody and guinea pig αCmi antibody (this study) at 1:1000 dilution overnight at 4°C. Samples were incubated with secondary antibodies Alexa Fluor 488 goat α-rabbit IgG and Alexa Fluor 568 goat α-guinea pig IgG (A11034 and A11075, ThermoFisher). Wing discs were mounted in ProLong Gold anti-fade reagent with DAPI (ThermoFisher). Polytene chromosome immunostaining was performed as described (46,54) with detection carried out using secondary antibodies as above diluted in block solution supplemented with 2% normal goat serum.

ChIP-sequencing

Chromatin collection and chromatin immunoprecipitation were performed as described previously (PMID: 21430782). Immunoprecipitated DNA was prepared for Illumina sequencing using the Epicentre Nextera DNA Sample Preparation Kit, using the High Molecular Weight tagmentation buffer. Tagmented DNA was amplified using 12 cycles of PCR and libraries were sequenced on an Illumina HiSeq 2000 according to manufacturer specifications. For data processing, ChIP and matched input control (from non-immunoprecipitated chromatin) sequencing data were aligned to the dm3 build of the Drosophila genome, and peaks were called using MACS version 2 with a *q*-value cutoff of 0.05 (PMID: 18798982). The embryo ChIP-seq peak calls were based on enrichment data from the strongest Cmi ChIP replicate in data previously published by the modENCODE project (GSE50365); the remaining S2 cell, W3L and WPP ChIP-seq data are available at GSE143747.

The overlap enrichment ratios and significance of overlap between genomic regions (ChIP peaks versus ChIP peaks or ChIP peaks versus chromatin states) were calculated using the mergePeaks program within the HOMER (Hypergeometric Optimization of Motif EnRichment) Suite (PMID: 20513432). STARR-seq data were used to identify enhancer regions with cell-specific or cell-shared activity based on data from [PMID: 23328393] and ecdysone-responsive activity based on data from [PMID: 24685159]. STARR-seq enhancers from [PMID: 23328393] were broken down into enhancers that are active in both S2 and OSC cells (Shared), enhancers active only in S2 cells (S2-specific), and enhancers active only in OSC cells (OSC-specific). STARR-seq enhancers from [PMID: 24685159] were broken down into ecdysone-induced enhancers (>2.5-fold higher STARR-seq signal in ecdysone versus control), ecdysone-repressed enhancers (>2.5-fold higher STARR-seq signal in control versus ecdysone), and constitutive enhancers (<2-fold difference in STARR-seq signal between control and ecdysone). Breakdown of binding events by genomic region was performed using the CEAS (*cis*-regulatory Element Annotation System) program within the Cistrome platform (PMID: 21859476). DNA conservation analysis was performed using the Cistrome's Conservation Plot tool. Motif enrichment analysis was performed using i-CisTarget (PMID: 22718975). Briefly, ChIP-seq peaks were scanned for enriched position weight matrices (PWMs) in i-CisTarget's version 2 PWM database. The top 5 non-redundant motifs associated with a possible Drosophila transcription factor are listed in Figure 4A. ChIP-seq data was plotted onto the dm3 genome build using the Integrated Genome Browser (IGB;(55)).When necessary, ChIP-seq data aligned to the dm3 genome (our results and data obtained from GEO and modENCODE databases, see Supplementary Table S2) were converted to align with the dm6 genome. The BED format was converted to be suitable for submission to the LiftOver software available at [https://genome.ucsc.edu/cgi-bin/hgLiftOver]. This conversion was carried out using this Python script: [https://github.com/dingwall-lab/COMPASS-like/blob/master/bed_to_liftover.py]. Next, BED files were compared with this Python script [https://github.com/dingwall-lab/COMPASS-like/blob/master/overlap_peaks.py] to find overlaps between peaks in different ChIP-seq files. Other ChIP-seq datasets used in this study are listed in Supplementary Table S2. We first determined the midpoint of each processed peak. Our python script would take two BED files, and an extension factor *n* bases. It takes the first BED file, extend all its peaks on both sides by *n* bases, then counts the number of peaks that overlap with those in the second BED file. In our figure (S7B), *n* was set at 2000 bases. For other analyses, peaks that overlapped would have midpoints that were within a certain base pair threshold (1000, 2500 and 5000 bp).

RESULTS

Cmi is dynamically enriched at enhancers and promoters

Genomic binding enrichments were determined for Cmi by ChIP-seq in Drosophila late embryo-derived S2 cells and various developmental stages to assess temporal targeting

of MLR complex functions. Concordant with estimates of 12–20 000 sites for KMT2C/D (18,19), ∼6000 Cmi enrichment sites were detected in S2 cells, predominantly on developmentally active (red) and housekeeping (yellow) genes (Figure 1A), and lower enrichments in chromatin associated with Polycomb (blue), HP1 (green) or constitutively repressed heterochromatin (black) (56). Localization relative to post-translational histone modifications and regulatory landscapes (8,57) revealed strong enrichments on chromatin marked by H3K4me1/me2 and H3K18ac/K27ac, as well as H3K4me2/me3 and H3K9ac, associated with transcriptional enhancers and promoters, respectively (Figure 1B). Consistent with enhancer regulation, Cmi localizes to active (open) enhancers identified by STARR-seq (self-transcribing active regulatory region sequencing (58)), characterized by the ability to drive transcription from a heterologous reporter and marked by H3K4me1 and H3K27ac (Figure 1C, Supplementary Figure S3C). Surprisingly, there is an inverse trend during animal development, with Cmi enrichments increasing on enhancers and decreasing on promoters (Supplementary Figure S4B).

While MLX complexes counteract Pc-G mediated repression (59), recent work suggested MLR complexes might play similar roles at some enhancers (19). In S2 cells, ∼50% of Pc-associated peaks were within 5 kb of a Cmi peak, suggesting possible co-regulation (Supplementary Table S3) (60). Cmi enrichments at different developmental stages in whole organisms (Supplementary Figure S3), including embryos (0–8 h after egg deposition), wandering third instar larvae (W3L) and white prepupae (WPP), demonstrated association with both PcG and HP1 bound chromatin to a larger extent than in S2 cells. Although our data is derived from whole animals rather than single cells, in both embryos and WPP, Cmi also shows modest enrichment on regions marked by the presence of H3K27me3 that are typically associated with poised gene enhancers (5). These findings are in accord with recently described functions of KMT2C/MLL3 in overcoming PcG-mediated transcriptional repression (19). Our results reveal that Cmi is predominantly enriched on gene enhancers and promoters, including both transcriptionally active and silent/poised enhancers, suggesting likely functions in regulating enhancers at different stages of activation.

We next analyzed the degree of overlap among Cmi enrichments at various developmental stages. Overall, the locations of Cmi binding peaks were distinctly different in embryos compared to S2 cells, with many embryonic enrichments not observed at the W3L and WPP stages (Figure 1D, Supplementary Figure S4A). The dynamic localization in response to developmental signals (Supplementary Figure S4B) suggests that binding had regressed at many embryonic sites, possibly reflecting enhancer decommissioning or changes in stage-specific chromatin interactions. While many Cmi peaks were shared between stages, the most significant overlaps were observed between W3L and WPP (Supplementary Figures S4 and S5), indicating that binding is strongly influenced by developmental context, with binding regions highly enriched for gene sets associated with metamorphosis (Figure 1E) and ecdysone hormone-responsive enhancers (61) (Figure 1F). Overall, these binding data are the first to reveal dynamic genome localization of the Cmi/MLR complex on enhancers and promoters in a developing organism.

MLR regulates hormone responsive enhancers

We identified substantial Cmi enrichment at late developmental stage ecdysone responsive enhancers and the MLR complex is required for the transactivation of EcR-USP target genes, likely through direct interactions (20,47). We chose to focus on the regions bound by Cmi uniquely at these stages (Figure 2A and B), but not in early embryos (0–8 h AEL). The ecdysone induced *Eip74EF* (E74) gene is essential for hormone-dependent transcription programming, oogenesis and autophagy and a homolog of mammalian *ELF2* that encodes an ETS-domain transcription factor important in regulating cellular signaling. The *Eip74EF* gene is activated by a hormone pulse in mid-embryogenesis (62) and again in late L3 clear-gut (CG) larvae in response to rising hormone titers (Figure 2C) and is activated by ecdysone in S2 cells. Cmi is not present at the *Eip74EF* locus in early embryos but is highly enriched at the W3L and WPP stages (Figure 2B), as well as in S2 cells. The large number of enrichment peaks within *Eip74EF* suggests the existence of multiple, possibly functionally redundant or additive transcriptional enhancers.

The induced expression of *Eip74EF* is dependent on the function of the MLR complex, as widespread shRNAi depletion of either *cmi* or *trr* resulted in reduced transcription (Figure 2D and E). *Eip74EF* transcription is strongly activated at the CG stage, while transcription decreases as hormone titers decrease in the WPP and EP stages (Figure 2D; see Figure 7A). Depletion of *cmi* or *trr* attenuated *Eip74EF* induction at the CG stage; however, unexpectedly resulted in elevated *Eip74EF* expression relative to the wild type level during the BG stage when hormone responsive genes are normally repressed (Figure 2E). In S2 cells and early W3L larvae Cmi is bound at multiple positions within the gene locus even though *Eip74EF* is not appreciably expressed. However, following activation (WPP) the Cmi binding peaks appear to match the S2 and W3L BG patterns with no obvious substantial rearrangement in response to hormone, suggesting that MLR complexes may act to monomethylate H3K4 at enhancers, and thus prime hormone responsive enhancers prior to activation. To address this possibility, we examined the co-localization of Cmi with other factors required for transcription induction in W3L larvae (BG) (Figure 2F). Cmi binding peaks strongly correlated with both H3K27ac and H3K4me1 at multiple positions (regions A-G) while RNAP II was present at low levels near the 3′ end and 5′ promoter region. We next tested whether the H3K4me1 mark was sensitive to loss of the complex in vivo (Figure 2G). Using shRNAi depletion in the posterior portion of the W3L wing imaginal disk (*en-Gal4>cmi-IR*) we found that loss of Cmi (left panel) corresponded with reduced H3K4me1 (right panel), revealing an unanticipated role for Cmi in the maintenance of the enhancer mark.

Our data suggests that the MLR complex likely primes hormone responsive enhancers at the *Eip74EF* locus in mid-embryogenesis and is required to maintain the inactive state until later stage re-activation. We tested this hypothesis by

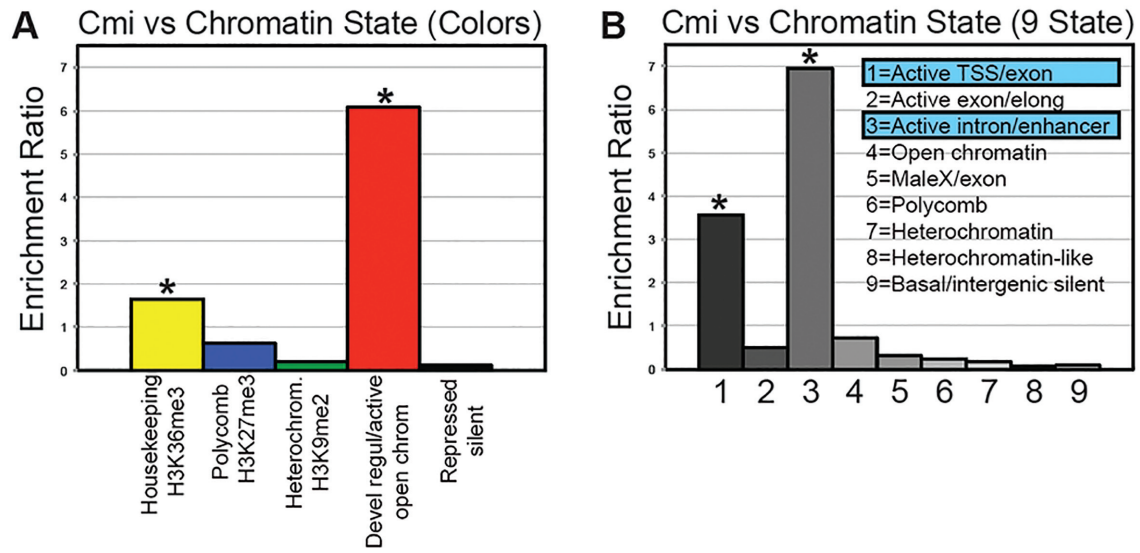

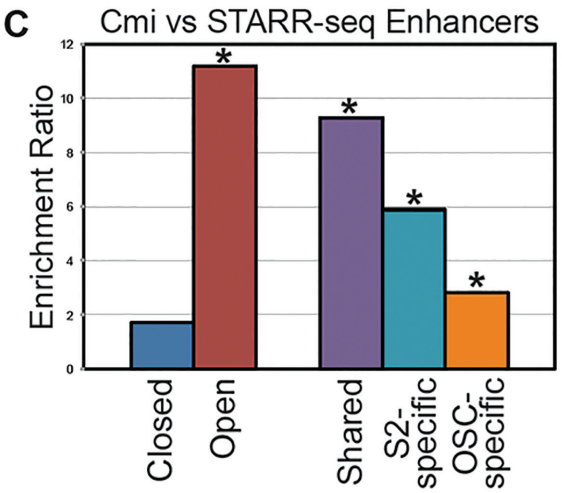

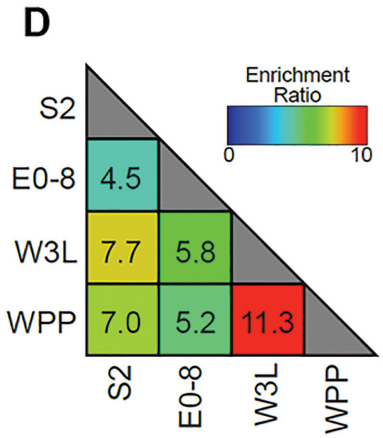

E

Annotation Cluster	Gene Ontology Term	p-value	Cluster Enrichment Score
1	Metamorphosis	4.97E-20	15.8
	Post-embryonic development	2.65E-18	
	Instar larval or pupal development	1.77E-18	
2	Cell motion	5.66E-12	8.5
	Cell morphogenesis	2.28E-10	
	Cellular component morphogenesis	7.26E-09	
3	Cell motion	5.66E-12	7.99
	Cell migration	1.87E-07	
	Cell motility	6.71E-07	
4	Gland development	4.22E-10	7.06
	Exocrine system development	1.62E-08	
	Salivary gland development	1.62E-08	
5	Morphogenesis of an epithelium	5.13E-09	6.34
	Tissue morphogenesis	1.44E-08	
	Epithelium development	2.95E-08	

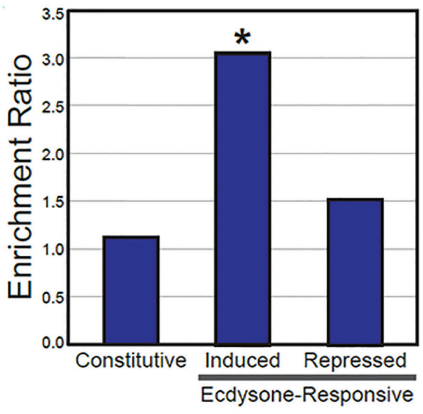

Figure 1. Cmi is enriched on active and inactive enhancers. ChIP-seq analyses of Cmi in Drosophila S2 cells. (**A**) Cmi is significantly associated with tissue-specific (red) and constitutively active genes (yellow) (56). (**B**) Cmi enrichment near transcription start sites (H3K4me2/me3, H3K9ac;State 1) and enhancers (H3K4me1, H3K18ac and H3K27ac;State 3) (57). (**C**) Cmi is highly enriched on active/open enhancers in multiple tissues (S2 and OSC cells) and tissue-specific enhancers based on STARR-seq analyses. (**D**) Cmi shows developmental stage-specific genome enrichments, with strong overlap between W3L and WPP and lower overlap between embryos (E0–8 h) and S2 cells. (**E**) Genes near W3L and WPP-specific binding regions are enriched for roles in metamorphosis and ecdysone-regulated processes. (**F**) Late stage (W3L and WPP) binding regions significantly overlap with ecdysone-induced enhancers.

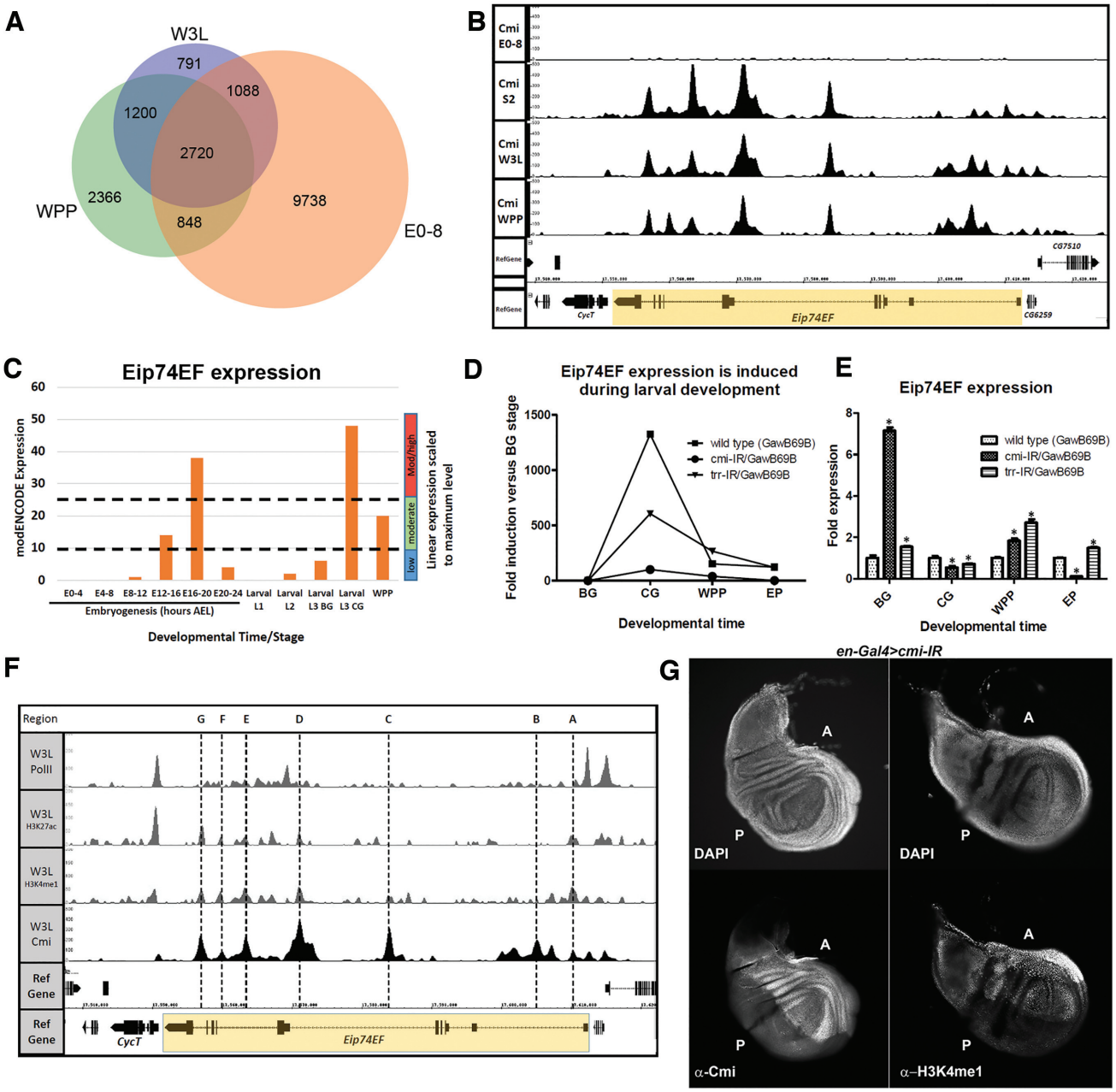

Figure 2. Cmi regulates ecdysone-dependent gene activation. (**A**) Venn diagram depiction of Cmi localization during development. ChIP enrichment peaks were compared between stages, with strongest overlap between the W3L and WPP stages. The majority of embryonic peaks (E0–8hrs) were not present at the later stages. (**B**) Developmentally dynamic enrichment of Cmi at multiple locations within the *Eip74EF* locus. Embryo 0–8 h (E0–8), S2 cells, wandering third instar larvae (W3L) and white prepupae (WPP). (**C**) *Eip74EF* transcription scaled to maximum expression (modENCODE) (112) coincides with ecdysone titers in embryos and late L3 larvae. (**D**) *Eip74EF* activation is reduced following Cmi or Trr shRNAi depletion during late larval development. RT-qPCR in wild type (*GawB69B-Gal4*) and knockdown of *cmi* and *trr* at the blue gut (BG), clear gut (CG), white prepupal (WPP) and early pupal (EP) stages (see Figure 7A for staging). Shown is the fold induction relative to the BG stage for each genotype. (**E**) Fold expression of *Eip74EF* relative to wild type (*GawB69B-Gal4*) at each developmental stage. (**F**) Localization of Cmi, H3K4me1, H3K27ac and RNAP II enrichments at the W3L stage. Recurrent Cmi enrichment regions (A-G) are indicated. (**G**) Cmi knockdown in the posterior (P) wing compartment (*en-Gal4>cmi-IR*) causes reductions in H3K4me1. Left panels, DAPI (top) and αCmi (bottom). Right panels, DAPI and αH3K4me1. **P*-value ≤0.05 by an unpaired Student's *t* test.

examining *Eip74EF* regulation in late embryo-derived S2 cells (+/−) ecdysone hormone (20-HE). Cmi (our data) and Trr (49) are enriched at genomic locations (A-G) that correspond with ecdysone responsive enhancers identified by STARR-seq (e1–e6; Figure 3A) including region D that displays both hormone dependent activation and repression functions, and two enhancers (A/e1 and E/e4) repressed in the presence of hormone (61). The ecdysone hormone response is mediated through enhancers/*cis*-regulatory modules that are located near ecdysone-responsive genes at variable distances that serve as binding sites for EcR/Usp, with or without hormone (61,63). Upon ligand/hormone binding, EcR leads to the activation of transcription, mediated through enhancer-promoter interactions. Some hormone response elements are indeed located near promoters, while others are not. In Drosophila, many such elements (e.g. EcR-response elements) are within introns, suggesting that they are enhancer, rather than promoter elements (61).

Since *Eip74EF* and other ecdysone-responsive genes are not transcribed in S2 cells without added hormone (41) there was no strong correspondence between H3K27ac enrichments and Cmi or Trr peaks. There was no detectable H3K9 or H3K27 methylation in this region (data not shown) indicating that the gene was not epigenetically repressed. While Cmi and Trr co-localize (Figure 3A), in contrast to late stage larvae (Figure 2F) the H3K4me1 enrichments in S2 cells were more widespread and adjacent to Cmi and Trr peaks, suggesting that the enhancers were already marked for activation in these cells perhaps in response to the earlier developmental pulse of hormone in mid-embryogenesis (62). The addition of 20-HE led to rapid induction of *Eip74EF* transcription (Figure 3B) that is dependent on Cmi (20). We verified co-localization of Cmi and Trr by ChIP-qPCR (+/−) hormone (Figure 3C). Surprisingly, both were reduced on regions A/e1, C/e3, D, E/e4 and G/e6 within 6 hours of hormone addition, indicating that transcript activation does not require 20-HE dependent recruitment or sustained binding of the Cmi-Trr/MLR complex at these enhancers, nor does the addition of hormone in this system significantly alter the epigenetic marks as they are already established.

We focused our analyses on enhancers activated in response to ecdysone (e1, e3, e4). While the localization of Cmi at these enhancers is dependent on the presence of Trr (Figure 3D), full Trr binding is retained at e3/e4 despite the depletion of Cmi and Trr binding at e1 appears to be sensitive to Cmi levels (Figure 3E). We next tested whether Cmi was important for the H3K4me1-associated with the Trr SET domain. While depletion of Cmi using RNAi in S2 cells resulted in significantly reduced H3K4me1 at the e1, e3 and e4 enhancers in the absence of ecdysone (Figure 3F), depletion of Trr showed only modest reduction of H3K4me1 under these conditions. In contrast, depletion of either Cmi or Trr led to a significant decrease in H3K4me1 (Figure 3G) and H3K27 acetylation (Figure 3H-I) at most enhancers following the addition of ecdysone, consistent with a reduced ability to activate *Eip74EF* transcription. Importantly, while the addition of hormone is required for activation, this occurs in the absence of newly deposited epigenetic marks, suggesting that the Cmi/Trr complex may contribute to a form of enhancer bookmarking. Our results are consistent with the hypothesis that Cmi is important to sustain the H3K4me1 enhancer mark placed by Trr prior to enhancer activation and possibly to re-establish the mark after the enhancer activation is completed and reset to a poised state (64).

MLR is an essential coactivator for developmental gene regulation

The Drosophila and mammalian MLR complexes serve as coactivators for multiple transcription factors including nuclear receptors. Genomic regions bound by Cmi at all stages are enriched for the GAGA/Trl motif as expected, while embryo-specific binding sites are highly enriched (*E*-score of 7.4) for the Zelda/Vfl pioneering transcription factor binding motif (CAGGTAG) (65). The differential binding at late larval (W3L) and early pupal (WPP) stages (Figure 1D) suggests Cmi might interact with factors controlling these stages with important roles in metamorphosis and hormone regulated processes (Figures 1E and 4A). The top enriched binding motifs include the Ecdysone receptor (EcR) and GATA-related motifs, with the top score (E-score 7.8) associated with the Grainyhead (Grh) transcription factor (66). To determine whether these motif enrichments were biologically significant, we examined the *Dopa decarboxylase (Ddc)* gene that is regulated by Grh through a consensus binding site near the *Ddc* promoter (Site I, Figure 4B) (67,68). Cmi displays modest binding at that site in later stages of development and none in embryos (Figure 4B), while Grh is highly enriched in embryos with reduced binding in wing imaginal discs (66). In contrast, both Cmi and Grh are highly enriched on the neighboring *brat (brain tumor)* gene at a consensus Grh target sequence (Site II). There is substantial overlap in the binding patterns within the *brat* gene at Grh peak regions (gray shaded boxes). The *Ddc* gene is activated at late larval stages coincident with rising titers of ecdysone (CG stage) but then declines at the onset of pupariation (Figure 4C). Widespread shRNAi depletion of *cmi, trr* or *grh* in late larvae attenuated transcription of *Ddc* (Figure 4D), indicating that the MLR complex is required for full *Ddc* activation. Similarly, the *brat* gene is activated at the CG stage (Figure 4E) and the induced transcription is blocked by depletion of *cmi, trr* and *grh* (Figure 4F). We next addressed whether Grh recruits or stabilizes the MLR complex on Grh target sites. Grh and Cmi binding was measured by ChIP-qPCR at Sites I and II in wild type and *grh-IR* larvae (Figure 4G). The low level of Cmi binding at Site I in the *Ddc* gene promoter was not appreciably altered upon loss of Grh despite reduced Grh at the site. In contrast, both Cmi and Grh binding were strongly reduced at Site II within the *brat* intron, suggesting that the Cmi-dependent regulation of *Ddc* expression may be through Cmi binding at enhancers within the *brat* gene. As both *Ddc* and *brat* are activated coincident with the onset of pupariation, we next asked whether the *Eip74EF* gene might also be subject to Grh regulation. Grh shows enriched binding at a Grh consensus site that coincides with Cmi binding region C in *Eip74EF* (Figure 2F, Supplementary Figure S6B). The expression of *Eip74EF* is sensitive to loss of *grh* (Supplementary Figure S4C) and both Grh and Cmi binding at

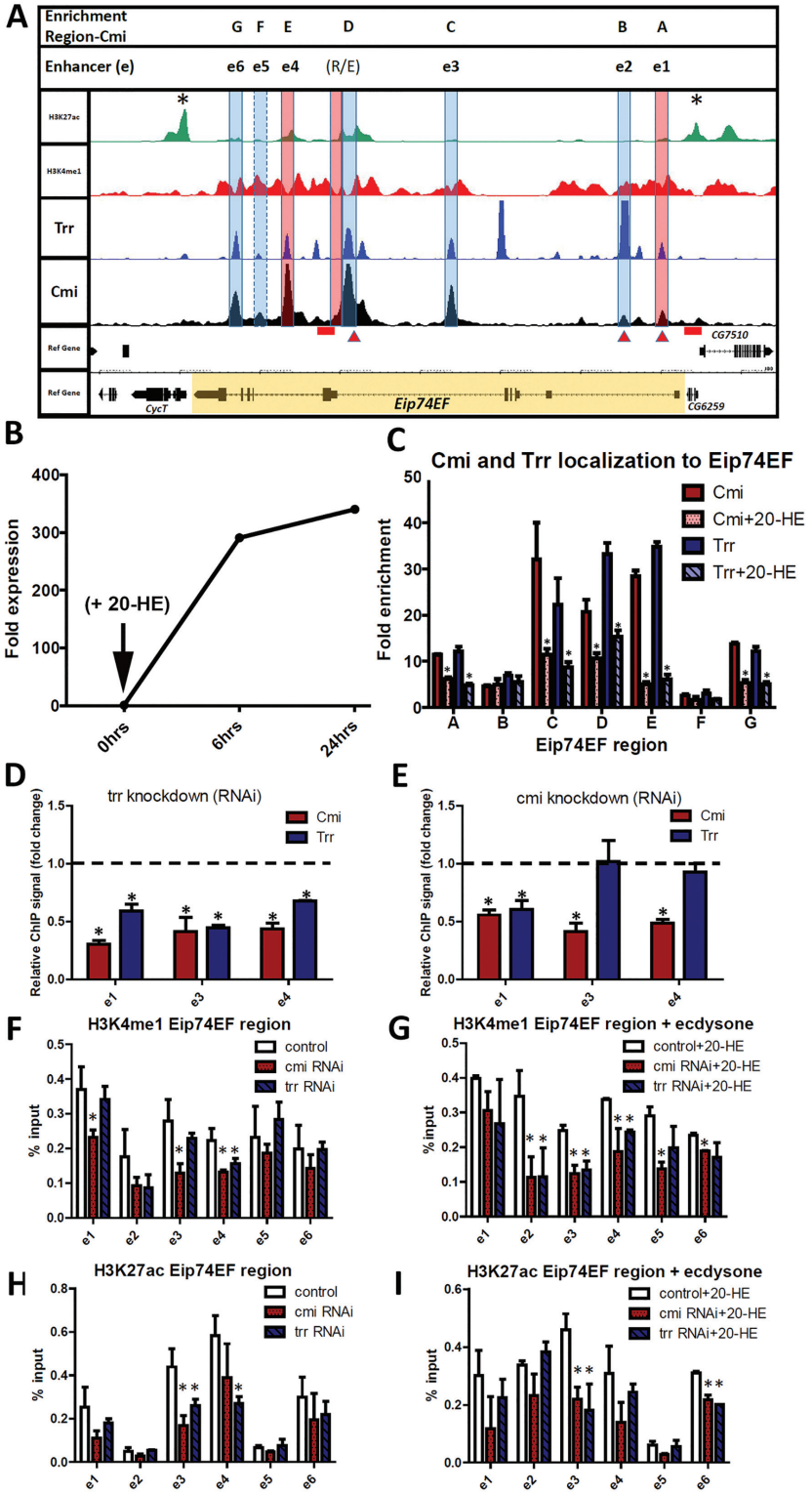

Figure 3. The Cmi/Trr complex regulates enhancer function. (**A**) Cmi and Trr co-localize on *Eip74EF* enhancers in S2 cells. Ecdysone responsive enhancers (e1–e6) were mapped by STARR-seq and DHS-seq, +/− ecdysone (61). Histone modifications H3K4me1, H3K27ac (modENCODE), Trr (49) and Cmi enrichments in S2 cells (regions A–G). Asterisks, positions of H3K4me3 peaks. Red bars below the Cmi track indicate locations of RNAP II. Region D contains both activation and repression functions (R/E). (**B**) *Eip74EF* transcription is induced by addition of 20-OH ecdysone (20-HE;1μM). (**C**) Co-localization of Cmi and Trr across the *Eip74EF* locus by ChIP-qPCR. Regions correspond to the major Cmi peaks (A–E). Enrichments are reduced at some locations upon addition of 20-HE for 6 h. (**D**, **E**) Enrichments of Cmi and Trr relative to normal S2 cells on the indicated enhancer regions following *trr* (D) and *cmi* knockdown (E). (**F–I**) Changes in H3K4me1 and H3K27ac enrichments at ecdysone responsive enhancers (e1–e6) normalized to histone H3 following *cmi* and *trr* knockdown, (+/−) 20-HE. H3K4me1 (F, G) and H3K27ac (H, I) are reduced on some enhancers following knockdown (–) 20-HE (F, H) and (+) 20-HE (G, I). **P*-value ≤0.05 by an unpaired Student's *t* test. Error bars represent mean ± SD.

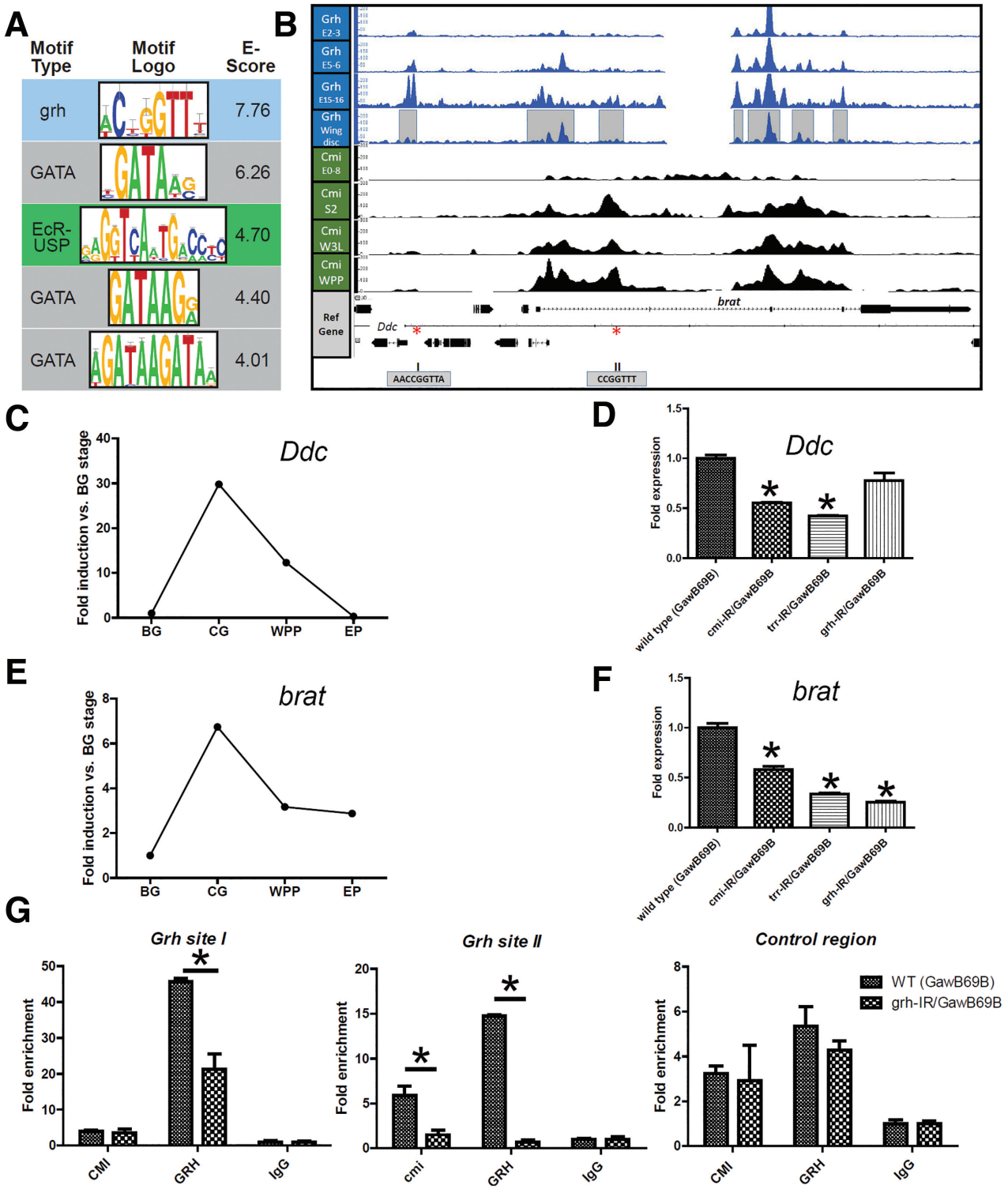

Figure 4. Cmi contributes to regulating Grainyhead (Grh) targets. (**A**) MOTIF analysis of Cmi enrichment regions exclusively in both W3L and WPP stages. Sequences and E-score (*P*-value multiplied by number of candidate sites) are shown. (**B**) Cmi co-localizes with Grh at known Grh targets (66). ChIP-seq data of Cmi and Grh enrichments near the *Ddc* locus. Grh ChIP-seq enrichments for embryonic times (E2-3hr, E5-6hr, E15-16hr after egg laying) and larval wing discs. Grey boxes represent called Grh peaks in wing discs. Locations of consensus Grh target sequences (I and II) are indicated by asterisks below the RefGene map. (**C**) *Ddc* expression corresponds to changes in ecdysone titers. Data are presented as fold induction relative to expression in the W3L blue gut (BG) stage. See Figure 7A for staging. (**D**) *Ddc* expression is regulated by Grh and the MLR complex. *Ddc* mRNA expression was measured at the CG stage upon knockdown of *cmi, trr* and *grh* using the *GawB69B-Gal4* driver. (**E**) *brat* mRNA expression is upregulated at the CG stage. (**F**) *brat* is positively regulated by Grh and the MLR complex at the CG stage of development. (**G**) Grh stabilizes Cmi at *Ddc* and *brat*. ChIP-qPCR analyses of Cmi and Grh enrichments at two Grh binding sites (I and II, panel B). Fold enrichments were assayed in control (*GawB69B-Gal4*) and *grh-IR* W3L CG larvae. A genomic region not containing Grh binding sites was used as a control. **P*-value ≤0.05 by an unpaired Student's *t* test.

that site are reduced when *grh* is depleted (Supplementary Figure S6D).

Grh has been shown to function as both an activator and a repressor of transcription (66,69–71). Strong overlap between Cmi and Grh binding at multiple developmental stages (Supplementary Figure S7) suggests that Grh may utilize the MLR complex as a coactivator or corepressor. In addition to co-localization and co-regulation of several common target genes, Cmi and Grh genetically interact in wing pattern development. Expression of an inverted repeat that depletes *grh* in the wing imaginal disc *(C765-Gal4>grh-IR)* leads to phenotypes similar to reduced *cmi* (20,22) (Supplementary Figure S8). In fact, simultaneous depletion of both leads to enhanced loss of wing vein development; while depletion of *grh* partially suppressed a *cmi* gain of function phenotype (Supplementary Table S4). We also found a general correspondence of common gene ontology groups among the genes in close proximity to Grh wing disc and Cmi W3L overlapping enrichment peaks that show reduced expression upon *grh* and *cmi* depletion in wing discs (Tables S5 and S6), suggesting functional co-localization. Finally, a recent study demonstrated direct contacts between mammalian GRHL2 and both KMT2C/D were important for NK-cell tumor killing functions (72), suggesting that MLR complexes are important co-regulators of GRH functions.

Cmi is important for MLR complex epigenetic functions

Cmi contains several conserved features including a cluster of plant homeodomain (PHD) histone recognition and binding zinc-fingers, a conserved HMG (high mobility group) domain, and nuclear receptor interaction motifs (LXXLL/LLXXL) (20). While Cmi levels decreased upon loss of Trr in S2 cells (Figure 3), we found Trr remained on *Eip74EF* gene enhancers when Cmi was depleted. Further, depletion of Cmi in S2 cells and larval wing discs led to decreased H3K4me1 (Figures 2,3). We addressed the function of Cmi within the MLR complex by determining the stability of the complex in the absence of Cmi protein. Extracts prepared from cmi^{1} null larvae (20) were probed by western blot with antibodies to Cmi, Trr and another complex component, Utx (Figure 5A). The Utx protein abundance was decreased concurrent with Cmi loss, although Trr was unaffected. Similarly, shRNAi *cmi* depletion revealed that Trr was present at normal levels (Figure 5B and C). Although Cmi protein stability is reduced when Trr is absent (Figure 5B), *cmi* transcript levels are unchanged (data not shown), suggesting that Cmi stability depends on the presence of Trr. While the mechanism of this instability is unknown, it may reflect Cmi degradation when it is unable to form MLR complexes (73,74).

To determine whether Cmi was required for Trr association with chromatin, we examined Cmi and Trr immunolocalization on polytene chromosomes when these proteins were removed by RNAi depletion using a salivary gland-specific Gal4 (*Sgs3-Gal4*). Depletion of Cmi or Trr led to the loss of Cmi staining on polytene chromosomes (Figure 5C, top), confirming that Cmi stability was reduced upon Trr loss. In contrast, loss of Cmi did not substantially affect Trr chromosome binding (Figure 5C, bottom), though there may be some Trr sites that are sensitive to Cmi loss; however, H3K4me1 was reduced (Figures 2G and 3F, G), suggesting that Cmi is either necessary for Trr dependent monomethylation of H3K4 or required to maintain the epigenetic mark, as Trr catalyzes H3K4me1 in the absence of Cmi *in vitro* (75,76) and Trr can potentially recruit CBP to acetylate H3K27 (49,75). We addressed these possibilities in two ways, using genetic removal of the H3K4 demethylases Lsd1/Su(var)3-3 and Lid/Kdm5 (77), and by examination of H3K27 acetylation by CBP. We previously found that Lsd1 functioned as a negative regulator of wing vein patterning in Drosophila (53,78). One possible mechanism may be through enhancer decommissioning (79) by removal of H3K4me1 marks. We hypothesized that if Cmi played a protective role in preventing enhancer decommissioning, then loss of Cmi function phenotypes would be suppressed by concurrent removal of Lsd1. Depletion of Cmi in the wing disc results in shortening of the L2 and L5 longitudinal veins (20) (Supplementary Figure S6B) through reduced activation of Dpp/Tgfβ signaling (22), while reduced Lsd1 function results in ectopic veins through deregulation of the same signaling pathway (78). We reasoned that if Cmi protected the H3K4me1, the *cmi-IR* shortened vein phenotype would be suppressed by simultaneously depleting Lsd1. We observed a slight enhancement (Supplementary Table S7) rather than suppression of the *cmi-IR* phenotype, suggesting that Cmi does not block the removal of the monomethyl mark. Conversely, Cmi might prevent the addition of H3K4me2/me3 marks. We tested for genetic interactions between *cmi* and the H3K4me2/3 demethylase *lid/Kdm5,* reasoning that if the *cmi* loss of function wing phenotype was coupled to increased H3K4 methylation, then loss of the H3K4me2/3 demethylase should enhance that phenotype (80–82). We tested two *lid-IR* lines and a strong loss of function *lid* mutant allele *(*lid^{k06801}*)* and found no obvious enhancement of the *cmi-IR* wing phenotype, while overexpression of active Lid/Kdm5 (42,81) strongly enhanced the phenotype (Supplementary Table S7). Thus, the *cmi-IR* loss of function phenotypes likely result from either reduced Trr-dependent H3K4 methylation or through other functions of the complex that are dependent on Cmi.

The presence of acetylated H3K27 is a common feature of active enhancers (5). In addition to decreased H3K4me1 upon loss or depletion of Cmi (Figures 2 and 3), we also observed reduced H3K27ac at the *Eip74EF* locus under both uninduced and induced (hormone stimulated) conditions in S2 cells (Figure 3H and I). Our results suggested that Cmi is important for enhancer H3K27ac through regulating the H3K4me1 activity of Trr or facilitating associations of CBP with the MLR complex. We first examined co-localization of CBP and H3K27ac marks with Cmi in late larvae (W3L) at ecdysone regulated loci and observed highly similar enrichments (Figure 6A), with ∼90% of CBP and over 70% of H3K27ac enrichment peaks within ±5 kb of Cmi peaks (Supplementary Table S8). Next, we confirmed in vivo association of CBP and Cmi by co-immunoprecipitation in embryo extracts using the HA-tagged Cmi (Figure 6B) (20). Current views suggest CBP is recruited to enhancers through interaction with Trr or by the presence of H3K4me1 (75). Since Trr protein is stable and bound to chromatin in the absence of Cmi, we

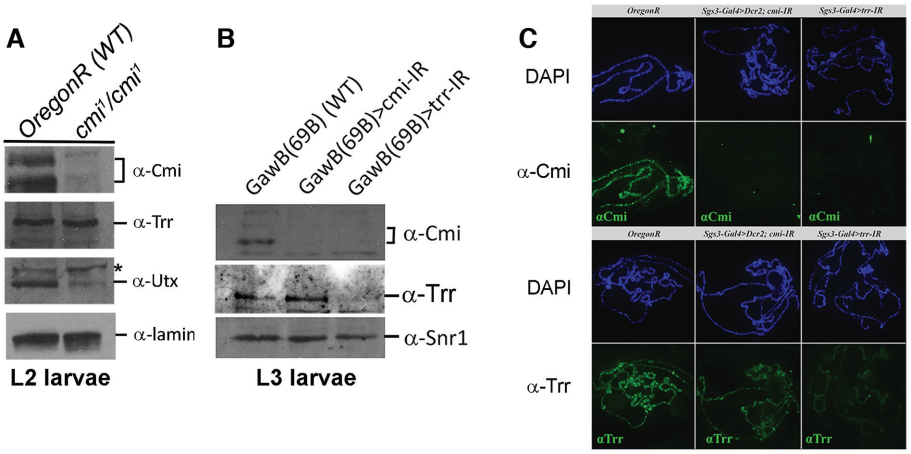

Figure 5. Cmi is not required for Trr binding. (**A**) Trr is stable in the absence of Cmi. Extracts from wild type (*OregonR*) and cmi^{1} homozygous null L2 larvae were probed for Cmi, Trr and Utx by immunoblotting, with α-Lamin as a control. *, non-specific (49). (**B**) Cmi stability is reduced upon loss of Trr. Immunoblots were probed for Cmi and Trr following knockdown in L3 larvae using *GawB69B-Gal4*. As a loading control, the extracts were probed for the expression of an unrelated protein, Snr1. (**C**) Polytene chromosome immunolocalization of Cmi and Trr following knockdown using the *Sgs3-Gal4* salivary gland driver. Chromosomes were visualized using DAPI.

tested whether H3K27ac would still occur. Depletion of Cmi in whole larvae using shRNAi led to reduced global H3K27 acetylation with a small increase in H3K27me3 levels by Western blot (Figure 6C); however, there was no substantial change in the transcription of *E(z),* encoding the H3K27 methyltransferase, or other PRC2 complex components (data not shown). These results raise the possibility that Cmi might have an important non-catalytic role in the recruitment or stable association of CBP on chromatin. To test this hypothesis, we depleted Cmi in salivary glands, examined polytene chromosomes and found greatly reduced global localization of CBP and H3K27ac (Figure 6D and E) with no obvious change in the level or distribution of H3K27me3 (Figure 6F).

The MLR complex has critical functions in both enhancer activation and repression

A critical role for MLR complexes in normal development and cancer (1) prompted us to next investigate the impacts on global gene expression associated with Cmi depletion, initially focusing on the larval CG stage coincident with elevated titers of hormone and transcriptome reprogramming (Figure 7A). RNA-seq analysis of wild type Drosophila revealed ∼3950 expressed genes (RPKM>1) that were upregulated at least 1.3-fold at the CG stage compared to the BG stage, while nearly 2700 were downregulated ($P \leq 0.05$). Upregulated genes were highly enriched for involvement in tissue morphogenesis and organ development, axon guidance, cell adhesion and cytoskeleton organization ($P \leq 5e{-}10$) and were more likely to reside within 10 kb of Cmi enrichment peaks (82.5% versus 68.6% for all genes, $P = 1.9e{-}61$) compared to downregulated genes (58.7%, $P = 1.5e{-}20$) that were enriched for involvement in proteolysis, antimicrobial defense, muscle contraction and chitin metabolism. Widespread shRNAi depletion of Cmi revealed that more genes were upregulated ($n = 3181$) than downregulated ($n = 1648$) at the CG stage compared to wild type. Genes responsive to hormone activation were prominent among downregulated transcripts (Supplementary Table S9); while upregulated genes were involved in a variety of metabolic processes (Supplementary Table S10). Our results suggest that the Drosophila MLR complex is critical for hormone-dependent transcription reprogramming at key developmental transitions.

Depletion of Cmi during the third larval instar blue gut (BG) stage resulted in an elevated transcription of *Eip74EF* (Figure 2E) despite low levels of ecdysone, suggesting that Cmi might be important for helping to silence a previously marked enhancer. To investigate this further, we performed RNAseq analyses of Cmi and Trr-depleted (Gal4-driven *cmi-IR, trr-IR*) Drosophila at different developmental stages (Figure 7A). Depletion of Cmi during the BG stage revealed approximately 3100 genes with increased expression (fold change ≥ 1.3, $P \leq 0.05$) relative to wild type animals, while nearly 1300 genes were downregulated at the subsequent CG stage (Figure 7B). Genes involved in variety of developmental and signaling processes showed increased transcription at the BG stage, while those with reduced transcription at the CG stage were largely involved in cuticle synthesis and metabolic pathways, processes related to metamorphosis (Figure 7C). Overall, 336 genes that showed elevated transcription at the BG stage showed reduced expression at the CG stage relative to wild type, indicating they are normally repressed or silenced when ecdysone titers are low but activated in response to ecdysone signaling that marks the transition into pupariation (83). Ontology analysis indicated that tissue development, cell adhesion, migration and metabolism genes were among the most affected targets upon Cmi depletion (Supplementary Table S11), as well as critical hormone response regulators including the *Eip* genes (*Eip63F-1*, *Eip74EF*, *Eip75B*, *Eip78C*) and other ligand dependent nuclear receptors that contribute to transcriptome and cellular reprogramming (Figure 7D). A similar trend was observed upon depletion of Trr (Supplementary Table S12), suggesting the MLR complex has essential functions in regulating enhancers that are activated or silenced at different developmental stages as part of larger

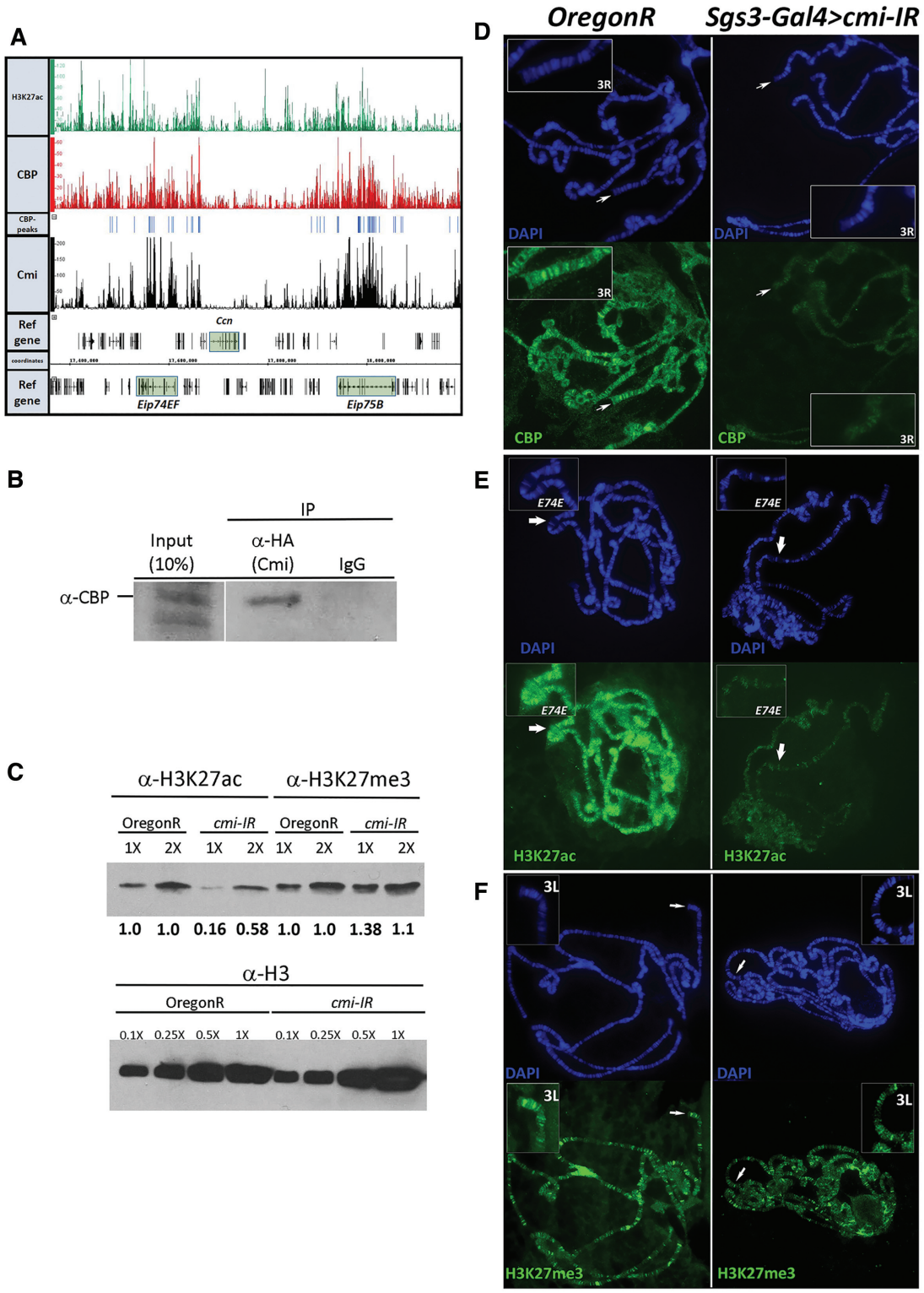

Figure 6. Cmi is required for stable CBP association and H3K27ac of chromatin. (**A**) ChIP-seq co-localization of Cmi, CBP and H3K27ac during the W3L stage in the chromosome region containing *Eip74EF* and *Eip75B*. (**B**) Cmi interacts with CBP by co-precipitation in vivo. Soluble nuclear lysates were prepared from embryos expressing an HA epitope-tagged Cmi (*GawB69B> UAS:HA-Cmi*) and αHA precipitated proteins were probed with αCBP antibodies. (**C**) Cmi is required for normal levels of H3K27 acetylation. Depletion of *cmi (GawB69B-Gal4>cmi-IR*) in W3L larvae is associated with reduced H3K27ac, but not H3K27me3. Native histone extracts were tested with αH3K27ac or αH3K27me3 by immunoblot. Controls for histone loading (0.1X to 1X) were examined using αH3. Band intensities were measured using Image J relative to the *OregonR* 1X level, normalized to H3 for each genotype. (D–F) Salivary gland polytene chromosomes from wild type *OregonR* or *Sgs3-Gal4>cmi-IR* knockdown larvae. Chromosomes were visualized by staining with DAPI. (**D**) CBP localization. Inset boxes show higher magnification views of chromosome 3R. (**E**) H3K27ac localization. Inset boxes are higher magnification views of the *Eip74EF* region. (**F**) H3K27me3 localization. Inset boxes are magnified views of chromosome 3L.

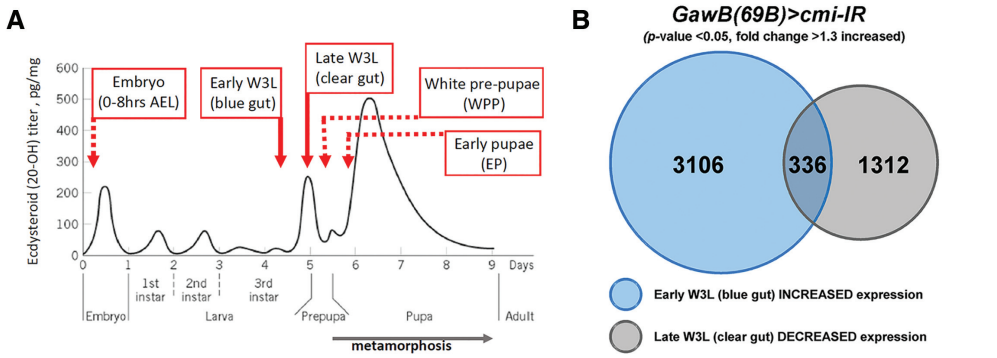

C

Cmi-IR vs. WT: Increased Early W3L (BG)			
Cellular Process	Gene Count	Fold enrichment	*p*-value
imaginal disc-derived wing morphogenesis	73	3.04	9.24E-19
protein phosphorylation	81	2.75	7.93E-18
axon guidance	60	2.93	1.28E-14
regulation of cell shape	43	3.70	1.35E-14
border follicle cell migration	44	3.03	1.78E-11
dorsal closure	38	3.33	2.31E-11
cell adhesion	35	3.36	1.20E-10
dendrite morphogenesis	52	2.55	2.70E-10
transcription, DNA-templated	81	1.94	4.17E-09
oogenesis	70	2.01	1.46E-08
JNK cascade	16	5.35	2.02E-08
determination of adult lifespan	43	2.28	3.51E-07

Cmi-IR vs. WT: Decreased Late W3L (CG)			
Cellular Process	Gene count	Fold enrichment	*p*-value
proteolysis	61	3.15	2.07E-15
chitin metabolic process	25	6.20	8.11E-13
oxidation-reduction process	41	2.44	2.60E-07
mesoderm development	12	4.60	4.69E-05
chitin catabolic process	7	6.87	4.00E-04
chitin-based cuticle development	17	2.62	7.42E-04
transmembrane transport	25	2.12	7.50E-04
hemolymph coagulation	5	10.23	1.03E-03
carbohydrate metabolic process	13	3.01	1.21E-03
de novo IMP biosynthetic process	4	16.36	1.22E-03
ecdysis, chitin-based cuticle	6	7.01	1.29E-03
myofibril assembly	5	8.18	2.57E-03

D

	Early W3L (BG)					Late W3L (CG)				
Gene Name	WT RPKM	Cmi RPKM	log2	fold	p-value	WT RPKM	Cmi RPKM	log2	fold	p-value
Eip63F-1	15.3	24.7	0.69	1.6	1.54E-68	35.2	22.2	-0.70	-1.6	3.35E-94
Eip74EF	13.6	18.7	0.46	1.4	3.18E-57	79.3	44.8	-0.80	-1.8	0.00E+00
Eip75B	7.6	13.8	0.86	1.8	1.98E-162	43.7	19.9	-1.14	-2.2	0.00E+00
Eip78C	0.8	1.8	1.20	2.3	7.78E-25	49	44.3	-0.15	-1.1	1.63E-15
br	22.9	38.4	0.75	1.7	0.00E+00	140	98.1	-0.51	-1.4	0.00E+00
brat	5.6	10.3	0.89	1.8	3.96E-188	40.7	37.4	-0.12	-1.1	1.01E-20

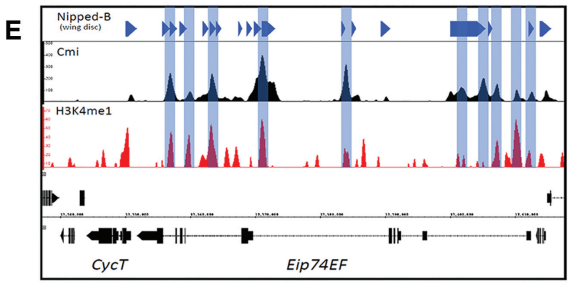

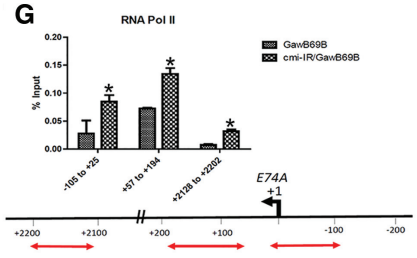

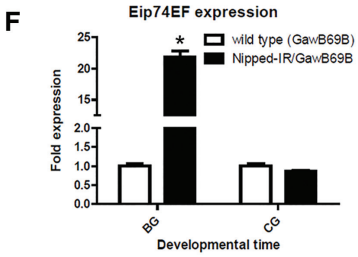

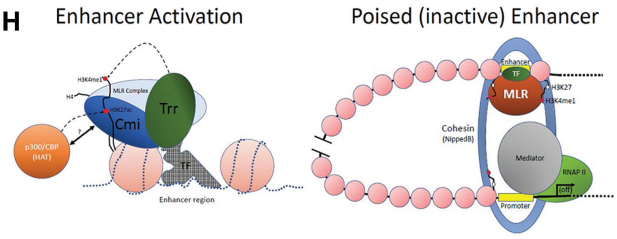

Figure 7. MLR regulates hormone-dependent enhancer activation and repression during development. (**A**) Cmi was depleted (*GawB69B-Gal4>cmi-IR)* and transcripts analyzed by RNAseq. Stages include W3L blue gut (BG; pre-ecdysone) and clear gut (CG; elevated ecdysone). Image modified from (113). (**B**) Venn diagram comparing changes in gene expression associated with *cmi* knockdown at the BG and CG stages. The analysis identified genes showing increased expression (*P*-value ≤ 0.05, fold change ≥ 1.3) compared to wild type (*GawB69B-Gal4*) at the BG stage that subsequently show reduced expression at the CG stage. (**C**) GO enrichment of the 336 genes shown in (B) filtered for RPKM values of ≥ 5 in wild type animals at each stage. GO groups are listed in descending order of *P*-value. (**D**) Cmi represses hormone responsive genes prior to activation. Ecdysone responsive genes show elevated BG expression upon *cmi* knockdown compared to wild type. Activation of these genes at the CG stage is attenuated when *cmi* is depleted. (**E**) Enrichment peak comparison of Cmi and H3K4me1 (whole W3L) with Nipped-B (wing discs). Co-localized peaks are highlighted in blue. (**F**) shRNAi depletion of *Nipped-B* results in derepression of *Eip74EF* at the BG stage. (**G**) Depletion of *Cmi* leads to increased RNAP II in the *Eip74EF* 5′ region (*E74A* promoter). (**H**) Two-stage model of MLR functions in enhancer activation and enhancer memory. (Left) Enhancer activation is associated with recruitment of the MLR complex to chromatin by sequence-specific transcription factors, monomethylation of H3K4 by Trr, recruitment or stabilization of CBP/p300 by Cmi and acetylation of H3K27. (Right) Previously active enhancers are maintained in an inactive or silenced (poised) state, stabilized by cohesin complexes and retaining the MLR complex in the absence of H3K27ac. See text for additional details.

gene regulatory networks that drive the proper timing and expression magnitude of genes important for developmental transitions.

Our RNAi depletion studies further revealed that developmental context is a major factor in transcriptome responses to loss of MLR complex function. Comparison of RNAseq results from Cmi depletion in pre- and post-ecdysone larvae showed that among the upregulated genes at both stages, nearly 375 genes are shared, including strong enrichment for genes involved in innate immunity and stress responses (Supplementary Table S13). Approximately 350 shared genes were downregulated at both stages and were highly enriched for functional roles in puparial adhesion, molting, innate immune responses and metabolism (Supplementary Table S14). These data suggest that there is a subset of genes that depend on the MLR complex for their enhancer activation or silencing, independent of hormone regulation.

The elevated transcription of hormone-inducible genes upon Cmi loss at the larval BG stage suggests that the complex might contribute to normal enhancer repression by facilitating long-range enhancer-promoter interaction (12,14,16,84) and chromatin domain organization, including RNAP II recruitment or stabilization of a paused polymerase (16,85,86). Cohesin binding helps to regulate long range enhancer-promoter communication and recruitment of cohesin at enhancers depends on MLR complex deposition of H3K4me1 (12,16,87–90). Nipped-B is required for cohesin binding to chromosomes (87) and it frequently co-localizes with Cmi at ∼80% overlap within a 5kb interval (Figure 7E), while RNAi depletion of *Nipped-B* in BG larvae results in derepression of *Eip74EF* transcription (Figure 7F). Consistent with strong genetic interaction, reduced *Nipped-B* in wing imaginal discs either using RNAi or loss-of-function mutations, enhanced the *cmi-IR* phenotype in the wing (Supplementary Figure S9). Examination of RNAP II localization by ChIP at the *Eip74EF* locus revealed increased enrichment of RNAP II at the promoter and first exon upon knockdown of Cmi at the BG stage consistent with the increased expression (Figure 7G). However, we were unable to detect significant changes in elongating polymerase. Altogether, our data supports the hypothesis that the increased expression upon MLR complex depletion was most likely associated with additional RNAP II recruitment and that the MLR complex may help to restrain RNAP II accumulation in the absence of strong activation signals, possibly through chromatin constraints mediated by cohesin/Nipped-B (91). These findings suggest that enhancer activity at the *Eip74EF* locus is sensitive to chromosome interactions facilitated through MLR complex functions.

We next determined whether the regulated genes were situated in close proximity (±5 kb) to Cmi enrichment peaks, as the majority of enhancers reside near their gene targets (92). Compared to all genes, those with increased expression associated with Cmi depletion in the larval BG stage were significantly (68% versus 53% for all genes; $P = 7.7e{-}41$) more likely to reside within 5 kb of a Cmi peak and even greater likelihood of being within 1 kb (48% versus 31%; $P = 3.2e{-}58$) (Supplementary Figure S10); however, genes showing decreased expression were significantly less likely to reside within 5 kb. Among the down-regulated genes, only 5% were associated with Cmi enrichments within ±200 bp of the transcript start site. This data is consistent with Cmi serving an essential function in regulating or enforcing the activation or repression of enhancer activities of genes that reside in close proximity to a binding peak.

DISCUSSION

We found that the Drosophila MLR complex is required not only for the *cis*-regulatory programming of enhancer functions but also for epigenetic maintenance of enhancer memory, supporting a model whereby the MLR complexes function in two distinct ways: contributing to enhancer commissioning and to marking (or bookmarking) enhancers to enable rapid transcriptional re-activation at subsequent developmental stages (Figure 7H).

Cmi exhibited a substantial genomic redistribution during development, likely in response to changing gene regulatory network controls that suggest functions in maintaining enhancer identity, as well as decommissioning. Cmi enrichments at genomic regions were associated with gene promoters and enhancers during early embryogenesis, with a significant trend towards enhancer binding at later stages, suggesting that developmental context is a critical determinant of MLR complex localization. This may reflect complex contributions to initial embryonic gene activation events through contact with promoters and enhancers via associations with pioneering transcription factors, such as grainyhead or Zelda/Vfl in Drosophila or FOXA1 in mammals (our results and (18,93)). After the initial activation of the ecdysone-dependent *Eip74EF* gene in mid/late embryos, the complex appears to remain enriched on regions associated with active and poised enhancers during the remainder of development, perhaps constrained or stabilized by long range enhancer/promoter chromatin interactions (14,94) initially formed during embryogenesis. Consistent with this view, MLR complexes have been associated with long range chromatin interactions (12,14,16), and the H3K4me1 mark contributes to recruitment of cohesin complexes (15) that are localized to topologically associating domain (TAD) boundaries. The formation of these large chromatin loops that involve *cis*-acting regulatory sequences are critical for properly regulating gene expression and the elaboration of cell differentiation programs (7,89,95–98). Altogether, our data supports the hypothesis that the MLR complexes play a significant role in establishing and maintaining *cis*-regulatory enhancer identity and function during animal development (Figure 7H).

Our model is further supported by examination of Cmi enrichments at enhancers in S2 cells and late larvae prior to increases in ecdysone titers that drive developmental transitions. At these stages/cells, the complex is enriched at enhancers in the *Eip74EF* gene occupied by EcR (94), marked with H3K4me1, low levels of H3K27ac and low or non-detectable transcription. Addition of hormone in S2 cells leads to Cmi-dependent rapid transcript activation without significant changes in histone marks or recruitment of additional MLR complexes (Figure 3). During activation, the MLR complex is reduced on some enhancers, perhaps reflecting an important step in subsequent re-setting of the

enhancer to a primed or poised state (93), concordant with our evidence that depletion of Cmi or Trr is associated with decreased H3K4me1 and H3K27ac and attenuated expression of *Eip74EF* upon addition of hormone (20), suggesting important MLR functions in maintaining enhancer identity in the absence of robust transcription. The histone binding PHD domains in Cmi may serve in an important role in establishing the H3K4me1 mark, as removal of Cmi leads to reduced H3K4me1 despite retention of Trr binding. Genetic removal of H3K4 demethylases *Lsd1* and *lid*/*Kdm5* did not significantly alter expression of *cmi-IR* phenotypes in the wing (20), implying that Cmi does not serve to protect the mark *per se*, but rather likely is important for promoting Trr methyltransferase function, possibly through facilitating Trr interactions with histone H3 tails (99).

While the MLR complex has essential functions coordinating enhancer activities within gene regulatory networks independent of hormone responsiveness, in the context of animal development the MLR complex contributes to the repression of hormone-dependent enhancer activation when ligands are at limiting levels. Depletion of Cmi and Trr in BG larvae, resulted in elevated transcription of several hormone-activated genes, consistent with our hypothesis that the complex has important roles in maintaining enhancer responsiveness during hormone-dependent genome reprogramming at developmental transition points. We found that a subset of developmental enhancers, those responsive to ecdysone hormone, are not regulated by Polycomb repressor complex (PRC2) associated H3K27me3; thus, the enhancers are activated and repressed by factors dependent on ecdysone levels. In the context of limiting (or absent) hormone during development, previously activated enhancers exist in a silent though primed or poised state, retain the H3K4me1 mark and are bound by transcription factors that partner with co-repressors to coordinate hormone-driven regulatory networks (83,100,101). Removal of Cmi or Trr results in a modest upregulation, implicating the complex in enforcing enhancer silencing, rather than through the removal of repressing histone marks via the H3K27 demethylase UTX. One possibility supported by our data is that the complex contributes to attenuating transcription when the induction signals are low or absent, perhaps indirectly through associations with cohesin/Nipped-B, as we observed increased transcription and RNAP II on the *Eip74EF* gene upon depletion of Cmi. The initial recruitment of MLR complexes to enhancers is required for RNAP II loading, eRNA synthesis and the subsequent recruitment of HAT enzymes (102). Surprisingly, once activated in animals, enhancers no longer require the presence of the H3K4me1 mark or the catalytic activity of Trr or KMT2C/D for survival to adulthood (11,12). Although the H3K4me1 mark itself is not required, we previously found using a null allele of *cmi* that homozygous loss led to larval lethality just prior to the major hormone peak that triggers metamorphosis (20), suggesting that Cmi is required for late enhancer functions beyond embryogenesis. Our current results support the hypothesis that Cmi is important for the recruitment or retention of CBP/p300 acetyltransferase and the H3K27ac mark that is essential for full enhancer activation. Since the PHD chromatin reader domain of Cmi or its vertebrate counterparts does not specifically recognize the H3K4me1 mark (20,99), it is possible that Cmi recognizes another chromatin feature, perhaps acetylated histone H4 (103), to help facilitate Trr methyltransferase activity and provide a bookmark of enhancer identity that allows for rapid re-activation upon inductive signaling.

Our results suggest a possible mechanism of MLR complex functions at developmental enhancers that relies on early transcription factor binding and recruitment of the MLR complex, which results in the H3K4me1 marking of those enhancers and activation through recruitment of CBP/p300 and H3K27 acetylation (Figure 7H). Our model is fully consistent with recent models of MLR complex functions in facilitating long range enhancer-promoter communication important for gene transcription (7,12,14,16). This hypothesis is further supported by several lines of evidence, including genetic interactions and co-localization of Cmi and Nipped-B, involved in cohesin complex formation and enhancer-promoter looping (91,104,105), as well as increased RNAP II at *Eip74EF* consistent with the up-regulation we observed with depletion of both Cmi and Nipped-B.

We also hypothesized that the retention of the complex at a subset of enhancers may provide a type of epigenetic memory and allow for rapid re-activation of those enhancers at later developmental stages. The presence of H3K4me1 together with either H3K27ac or H3K27me3, is generally considered a hallmark of enhancers (106). These as well as other epigenetic marks appear to be stable during mitosis (107). Epigenetic stability is a form of mitotic bookmarking that allows for somatic heritability of gene expression patterns following cell division, in some cases allowing for rapid re-activation in early G1 phase (108,109). In this regard, certain epigenetic marks and transcription factors remain associated with mitotic chromatin, thereby locking in transcriptional states and serving to block the spread of active/repressive states from neighboring genomic regions (107). A recent comprehensive study examined global histone modifications and chromatin dynamics in both interphase and mitotic cells and concluded that many genomic features were unchanged between these stages (110), with stable global levels and localized enrichments of histone methylation and slightly diminished histone acetylation. Epigenetic co-factors including KMT2A/MLL1, CBP/p300 and acetyl lysine binding protein BRD4 (111) are retained on mitotic chromatin suggesting important roles in chromatin bookmarking. Both CBP/p300 and BRD4 are recruited to chromatin through association with mammalian MLR complexes (18).

Our data, including the first developmental profile of MLR chromatin enrichment, provides strong support for this two-stage model of MLR complex functions, allowing for the prediction that loss of the MLR complexes in undifferentiated or somatic cells could cause a failure to activate specific developmental programs and lead to inappropriate regulation of enhancers, resulting in an oncogenic event. The large number of cancers associated with both KMT2C and KMT2D loss (1) and the critical importance of these proteins in development, cell differentiation and reprogramming (18), provides a strong rationale for further exploration of the MLR complex functions in normal animal development.

DATA AVAILABILITY

GEO Accession Numbers: RNA sequencing GSE143239; ChIP sequencing GSE50365, GSE143747; Data analysis: https://github.com/dingwall-lab/COMPASS-like/blob/master/filter.py, https://github.com/dingwall-lab/COMPASS-like/blob/master/count_like_terms.py, https://github.com/dingwall-lab/COMPASS-like/blob/master/venn_diagram.py, https://github.com/dingwall-lab/COMPASS-like/blob/master/bed_to_liftover.py, https://github.com/dingwall-lab/COMPASS-like/blob/master/overlap_peaks.py.

SUPPLEMENTARY DATA

Supplementary Data are available at NAR Online.

ACKNOWLEDGEMENTS

The authors wish to thank Christine Nguyen for help with genetic sorting and Lijia Ma and Alec Victorsen for help with ChIP-seq data process. The authors would also like to thank Manuel Diaz, David Ford, Tim Nickels, Maria Figueroa and Eileen Furlong for helpful discussions and advice.

FUNDING

National Institutes of Health [R35GM119553 to M.S.]; National Science Foundation [MCB-1413331, MCB-1716431 to A.K.D.]; the modERN Project generated the ChIP-seq data for Cmi, supported by a grant from the National Institutes of Health [U41HG007355 to K.P.W.]; Stocks obtained from the Bloomington Drosophila Stock Center [NIH P40OD018537]. Funding for open access charge: National Science Foundation [MCB 1716431].
Conflict of interest statement. None declared.

REFERENCES

1. Fagan,R.J. and Dingwall,A.K. (2019) COMPASS ascending: emerging clues regarding the roles of MLL3/KMT2C and MLL2/KMT2D proteins in cancer. *Cancer Lett.*, **458**, 56–65.
2. Shilatifard,A. (2012) The COMPASS family of histone H3K4 methylases: mechanisms of regulation in development and disease pathogenesis. *Annu. Rev. Biochem.*, **81**, 65–95.
3. Stathopoulos,A. and Levine,M. (2005) Genomic regulatory networks and animal development. *Dev. Cell*, **9**, 449–462.
4. Slattery,M., Zhou,T., Yang,L., Dantas Machado,A.C., Gordan,R. and Rohs,R. (2014) Absence of a simple code: how transcription factors read the genome. *Trends Biochem. Sci.*, **39**, 381–399.
5. Calo,E. and Wysocka,J. (2013) Modification of enhancer chromatin: what, how, and why? *Mol. Cell*, **49**, 825–837.
6. Rothbart,S.B. and Strahl,B.D. (2014) Interpreting the language of histone and DNA modifications. *Biochim. Biophys. Acta*, **1839**, 627–643.
7. Rickels,R. and Shilatifard,A. (2018) Enhancer logic and mechanics in development and disease. *Trends Cell Biol.*, **28**, 608–630.
8. Roy,S., Ernst,J., Kharchenko,P.V., Kheradpour,P., Negre,N., Eaton,M.L., Landolin,J.M., Bristow,C.A., Ma,L., Lin,M.F. *et al.* (2010) Identification of functional elements and regulatory circuits by Drosophila modENCODE. *Science*, **330**, 1787–1797.
9. Heintzman,N.D., Hon,G.C., Hawkins,R.D., Kheradpour,P., Stark,A., Harp,L.F., Ye,Z., Lee,L.K., Stuart,R.K., Ching,C.W. *et al.* (2009) Histone modifications at human enhancers reflect global cell-type-specific gene expression. *Nature*, **459**, 108–112.
10. Heintzman,N.D., Stuart,R.K., Hon,G., Fu,Y., Ching,C.W., Hawkins,R.D., Barrera,L.O., Van Calcar,S., Qu,C., Ching,K.A. *et al.* (2007) Distinct and predictive chromatin signatures of transcriptional promoters and enhancers in the human genome. *Nat. Genet.*, **39**, 311–318.
11. Dorighi,K.M., Swigut,T., Henriques,T., Bhanu,N.V., Scruggs,B.S., Nady,N., Still,C.D. 2nd, Garcia,B.A., Adelman,K. and Wysocka,J. (2017) Mll3 and Mll4 facilitate enhancer RNA synthesis and transcription from promoters independently of H3K4 monomethylation. *Mol. Cell*, **66**, 568–576.
12. Rickels,R., Herz,H.M., Sze,C.C., Cao,K., Morgan,M.A., Collings,C.K., Gause,M., Takahashi,Y.H., Wang,L., Rendleman,E.J. *et al.* (2017) Histone H3K4 monomethylation catalyzed by Trr and mammalian COMPASS-like proteins at enhancers is dispensable for development and viability. *Nat. Genet.*, **49**, 1647–1653.
13. Wang,S.P., Tang,Z., Chen,C.W., Shimada,M., Koche,R.P., Wang,L.H., Nakadai,T., Chramiec,A., Krivtsov,A.V., Armstrong,S.A. *et al.* (2017) A UTX-MLL4-p300 transcriptional regulatory network coordinately shapes active enhancer landscapes for eliciting transcription. *Mol. Cell*, **67**, 308–321.
14. Placek,K., Hu,G., Cui,K., Zhang,D., Ding,Y., Lee,J.E., Jang,Y., Wang,C., Konkel,J.E., Song,J. *et al.* (2017) MLL4 prepares the enhancer landscape for Foxp3 induction via chromatin looping. *Nat. Immunol.*, **18**, 1035–1045.
15. Baas,R., van Teeffelen,H., Tjalsma,S.J.D. and Timmers,H.T.M. (2018) The mixed lineage leukemia 4 (MLL4) methyltransferase complex is involved in transforming growth factor beta (TGF-beta)-activated gene transcription. *Transcription*, **9**, 67–74.
16. Yan,J., Chen,S.A., Local,A., Liu,T., Qiu,Y., Dorighi,K.M., Preissl,S., Rivera,C.M., Wang,C., Ye,Z. *et al.* (2018) Histone H3 lysine 4 monomethylation modulates long-range chromatin interactions at enhancers. *Cell Res.*, **28**, 204–220.
17. Lee,J.E., Wang,C., Xu,S., Cho,Y.W., Wang,L., Feng,X., Baldridge,A., Sartorelli,V., Zhuang,L., Peng,W. *et al.* (2013) H3K4 mono- and di-methyltransferase MLL4 is required for enhancer activation during cell differentiation. *Elife*, **2**, e01503.
18. Wang,C., Lee,J.E., Lai,B., Macfarlan,T.S., Xu,S., Zhuang,L., Liu,C., Peng,W. and Ge,K. (2016) Enhancer priming by H3K4 methyltransferase MLL4 controls cell fate transition. *Proc. Natl. Acad. Sci. U.S.A.*, **113**, 11871–11876.
19. Wang,L., Zhao,Z., Ozark,P.A., Fantini,D., Marshall,S.A., Rendleman,E.J., Cozzolino,K.A., Louis,N., He,X., Morgan,M.A. *et al.* (2018) Resetting the epigenetic balance of Polycomb and COMPASS function at enhancers for cancer therapy. *Nat. Med.*, **24**, 758–769.
20. Chauhan,C., Zraly,C.B., Parilla,M., Diaz,M.O. and Dingwall,A.K. (2012) Histone recognition and nuclear receptor co-activator functions of Drosophila Cara Mitad, a homolog of the N-terminal portion of mammalian MLL2 and MLL3. *Development*, **139**, 1997–2008.
21. Ali,M., Hom,R.A., Blakeslee,W., Ikenouye,L. and Kutateladze,T.G. (2014) Diverse functions of PHD fingers of the MLL/KMT2 subfamily. *Biochim. Biophys. Acta*, **1843**, 366–371.
22. Chauhan,C., Zraly,C.B. and Dingwall,A.K. (2013) The Drosophila COMPASS-like Cmi-Trr coactivator complex regulates dpp/BMP signaling in pattern formation. *Dev. Biol.*, **380**, 185–198.
23. Mohan,M., Herz,H.M., Smith,E.R., Zhang,Y., Jackson,J., Washburn,M.P., Florens,L., Eissenberg,J.C. and Shilatifard,A. (2011) The COMPASS family of H3K4 methylases in Drosophila. *Mol. Cell. Biol.*, **31**, 4310–4318.
24. Kanda,H., Nguyen,A., Chen,L., Okano,H. and Hariharan,I.K. (2013) The Drosophila ortholog of MLL3 and MLL4, trithorax related, functions as a negative regulator of tissue growth. *Mol. Cell. Biol.*, **33**, 1702–1710.
25. Oh,H., Slattery,M., Ma,L., Crofts,A., White,K.P., Mann,R.S. and Irvine,K.D. (2013) Genome-wide association of Yorkie with chromatin and chromatin-remodeling complexes. *Cell Rep.*, **3**, 309–318.
26. Qing,Y., Yin,F., Wang,W., Zheng,Y., Guo,P., Schozer,F., Deng,H. and Pan,D. (2014) The Hippo effector Yorkie activates transcription by interacting with a histone methyltransferase complex through Ncoa6. *Elife*, **3**, e02564.

27. Rhee,C., Lee,B.K., Beck,S., LeBlanc,L., Tucker,H.O. and Kim,J. (2017) Mechanisms of transcription factor-mediated direct reprogramming of mouse embryonic stem cells to trophoblast stem-like cells. *Nucleic Acids Res.*, **45**, 10103–10114.
28. Li,T. and Kelly,W.G. (2011) A role for Set1/MLL-related components in epigenetic regulation of the *Caenorhabditis elegans* germ line. *PLos Genet.*, **7**, e1001349.
29. Aoshima,K., Inoue,E., Sawa,H. and Okada,Y. (2015) Paternal H3K4 methylation is required for minor zygotic gene activation and early mouse embryonic development. *EMBO Rep.*, **16**, 803–812.
30. Faundes,V., Malone,G., Newman,W.G. and Banka,S. (2019) A comparative analysis of KMT2D missense variants in Kabuki syndrome, cancers and the general population. *J. Hum. Genet.*, **64**, 161–170.
31. Ford,D.J. and Dingwall,A.K. (2015) The cancer COMPASS: navigating the functions of MLL complexes in cancer. *Cancer Genet*, **208**, 178–191.
32. Froimchuk,E., Jang,Y. and Ge,K. (2017) Histone H3 lysine 4 methyltransferase KMT2D. *Gene*, **627**, 337–342.
33. Lee,J., Saha,P.K., Yang,Q.H., Lee,S., Park,J.Y., Suh,Y., Lee,S.K., Chan,L., Roeder,R.G. and Lee,J.W. (2008) Targeted inactivation of MLL3 histone H3-Lys-4 methyltransferase activity in the mouse reveals vital roles for MLL3 in adipogenesis. *Proc. Natl. Acad. Sci. U.S.A.*, **105**, 19229–19234.
34. Lee,S., Lee,J., Lee,S.K. and Lee,J.W. (2008) Activating signal cointegrator-2 is an essential adaptor to recruit histone H3 lysine 4 methyltransferases MLL3 and MLL4 to the liver X receptors. *Mol. Endocrinol.*, **22**, 1312–1319.
35. Yang,W. and Ernst,P. (2017) Distinct functions of histone H3, lysine 4 methyltransferases in normal and malignant hematopoiesis. *Curr. Opin. Hematol.*, **24**, 322–328.
36. Van Laarhoven,P.M., Neitzel,L.R., Quintana,A.M., Geiger,E.A., Zackai,E.H., Clouthier,D.E., Artinger,K.B., Ming,J.E. and Shaikh,T.H. (2015) Kabuki syndrome genes KMT2D and KDM6A: functional analyses demonstrate critical roles in craniofacial, heart and brain development. *Hum. Mol. Genet.*, **24**, 4443–4453.
37. Kleefstra,T., Kramer,J.M., Neveling,K., Willemsen,M.H., Koemans,T.S., Vissers,L.E., Wissink-Lindhout,W., Fenckova,M., van den Akker,W.M., Kasri,N.N. *et al.* (2012) Disruption of an EHMT1-associated chromatin-modification module causes intellectual disability. *Am. J. Hum. Genet.*, **91**, 73–82.
38. Koemans,T.S., Kleefstra,T., Chubak,M.C., Stone,M.H., Reijnders,M.R.F., de Munnik,S., Willemsen,M.H., Fenckova,M., Stumpel,C., Bok,L.A. *et al.* (2017) Functional convergence of histone methyltransferases EHMT1 and KMT2C involved in intellectual disability and autism spectrum disorder. *PLos Genet.*, **13**, e1006864.
39. Lintas,C. and Persico,A.M. (2018) Unraveling molecular pathways shared by Kabuki and Kabuki-like syndromes. *Clin. Genet.*, **94**, 283–295.
40. Rao,R.C. and Dou,Y. (2015) Hijacked in cancer: the KMT2 (MLL) family of methyltransferases. *Nat. Rev. Cancer*, **15**, 334–346.
41. Zraly,C.B., Middleton,F.A. and Dingwall,A.K. (2006) Hormone-response genes are direct in vivo regulatory targets of Brahma (SWI/SNF) complex function. *J. Biol. Chem.*, **281**, 35305–35315.
42. Liu,X. and Secombe,J. (2015) The histone demethylase KDM5 activates gene expression by recognizing chromatin context through its PHD reader motif. *Cell Rep.*, **13**, 2219–2231.
43. Bainbridge,S.P. and Bownes,M. (1981) Staging the metamorphosis of *Drosophila melanogaster*. *J. Embryol. Exp. Morphol.*, **66**, 57–80.
44. Andres,A.J. and Thummel,C.S. (1994) Methods for quantitative analysis of transcription in larvae and prepupae. *Methods Cell Biol.*, **44**, 565–573.
45. Negre,N., Lavrov,S., Hennetin,J., Bellis,M. and Cavalli,G. (2006) Mapping the distribution of chromatin proteins by ChIP on chip. *Methods Enzymol.*, **410**, 316–341.
46. Zraly,C.B., Marenda,D.R., Nanchal,R., Cavalli,G., Muchardt,C. and Dingwall,A.K. (2003) SNR1 is an essential subunit in a subset of Drosophila Brm complexes, targeting specific functions during development. *Dev. Biol.*, **253**, 291–308.
47. Sedkov,Y., Cho,E., Petruk,S., Cherbas,L., Smith,S.T., Jones,R.S., Cherbas,P., Canaani,E., Jaynes,J.B. and Mazo,A. (2003) Methylation at lysine 4 of histone H3 in ecdysone-dependent development of Drosophila. *Nature*, **426**, 78–83.
48. Herz,H.M., Madden,L.D., Chen,Z., Bolduc,C., Buff,E., Gupta,R., Davuluri,R., Shilatifard,A., Hariharan,I.K. and Bergmann,A. (2010) The H3K27me3 demethylase dUTX is a suppressor of Notch- and Rb-dependent tumors in Drosophila. *Mol. Cell Biol.*, **30**, 2485–2497.
49. Herz,H.M., Mohan,M., Garruss,A.S., Liang,K., Takahashi,Y.H., Mickey,K., Voets,O., Verrijzer,C.P. and Shilatifard,A. (2012) Enhancer-associated H3K4 monomethylation by Trithorax-related, the Drosophila homolog of mammalian Mll3/Mll4. *Genes Dev.*, **26**, 2604–2620.
50. Tie,F., Banerjee,R., Stratton,C.A., Prasad-Sinha,J., Stepanik,V., Zlobin,A., Diaz,M.O., Scacheri,P.C. and Harte,P.J. (2009) CBP-mediated acetylation of histone H3 lysine 27 antagonizes Drosophila Polycomb silencing. *Development*, **136**, 3131–3141.
51. Harrison,M.M., Botchan,M.R. and Cline,T.W. (2010) Grainyhead and Zelda compete for binding to the promoters of the earliest-expressed Drosophila genes. *Dev. Biol.*, **345**, 248–255.
52. Weake,V.M., Dyer,J.O., Seidel,C., Box,A., Swanson,S.K., Peak,A., Florens,L., Washburn,M.P., Abmayr,S.M. and Workman,J.L. (2011) Post-transcription initiation function of the ubiquitous SAGA complex in tissue-specific gene activation. *Genes Dev.*, **25**, 1499–1509.
53. Curtis,B.J., Zraly,C.B., Marenda,D.R. and Dingwall,A.K. (2011) Histone lysine demethylases function as co-repressors of SWI/SNF remodeling activities during Drosophila wing development. *Dev. Biol.*, **350**, 534–547.
54. Paro,R. (2008) Mapping protein distributions on polytene chromosomes by immunostaining. *CSH Protoc.*, **2008**, doi:10.1101/pdb.prot4714.
55. Freese,N.H., Norris,D.C. and Loraine,A.E. (2016) Integrated genome browser: visual analytics platform for genomics. *Bioinformatics*, **32**, 2089–2095.
56. Filion,G.J., van Bemmel,J.G., Braunschweig,U., Talhout,W., Kind,J., Ward,L.D., Brugman,W., de Castro,I.J., Kerkhoven,R.M., Bussemaker,H.J. *et al.* (2010) Systematic protein location mapping reveals five principal chromatin types in Drosophila cells. *Cell*, **143**, 212–224.
57. Kharchenko,P.V., Alekseyenko,A.A., Schwartz,Y.B., Minoda,A., Riddle,N.C., Ernst,J., Sabo,P.J., Larschan,E., Gorchakov,A.A., Gu,T. *et al.* (2011) Comprehensive analysis of the chromatin landscape in Drosophila melanogaster. *Nature*, **471**, 480–485.
58. Arnold,C.D., Gerlach,D., Stelzer,C., Boryn,L.M., Rath,M. and Stark,A. (2013) Genome-wide quantitative enhancer activity maps identified by STARR-seq. *Science*, **339**, 1074–1077.
59. Schuettengruber,B., Chourrout,D., Vervoort,M., Leblanc,B. and Cavalli,G. (2007) Genome regulation by polycomb and trithorax proteins. *Cell*, **128**, 735–745.
60. Rickels,R., Hu,D., Collings,C.K., Woodfin,A.R., Piunti,A., Mohan,M., Herz,H.M., Kvon,E. and Shilatifard,A. (2016) An evolutionary conserved epigenetic mark of polycomb response elements implemented by Trx/MLL/COMPASS. *Mol. Cell*, **63**, 318–328.
61. Shlyueva,D., Stelzer,C., Gerlach,D., Yanez-Cuna,J.O., Rath,M., Boryn,L.M., Arnold,C.D. and Stark,A. (2014) Hormone-responsive enhancer-activity maps reveal predictive motifs, indirect repression, and targeting of closed chromatin. *Mol. Cell*, **54**, 180–192.
62. Kozlova,T. and Thummel,C.S. (2003) Essential roles for ecdysone signaling during Drosophila mid-embryonic development. *Science*, **301**, 1911–1914.
63. Gauhar,Z., Sun,L.V., Hua,S., Mason,C.E., Fuchs,F., Li,T.R., Boutros,M. and White,K.P. (2009) Genomic mapping of binding regions for the Ecdysone receptor protein complex. *Genome Res.*, **19**, 1006–1013.
64. Ostuni,R., Piccolo,V., Barozzi,I., Polletti,S., Termanini,A., Bonifacio,S., Curina,A., Prosperini,E., Ghisletti,S. and Natoli,G. (2013) Latent enhancers activated by stimulation in differentiated cells. *Cell*, **152**, 157–171.
65. Schulz,K.N., Bondra,E.R., Moshe,A., Villalta,J.E., Lieb,J.D., Kaplan,T., McKay,D.J. and Harrison,M.M. (2015) Zelda is differentially required for chromatin accessibility, transcription factor binding, and gene expression in the early Drosophila embryo. *Genome Res.*, **25**, 1715–1726.

66. Nevil,M., Bondra,E.R., Schulz,K.N., Kaplan,T. and Harrison,M.M. (2017) Stable binding of the conserved transcription factor grainy head to its target genes throughout Drosophila melanogaster development. *Genetics*, **205**, 605–620.
67. Uv,A.E., Thompson,C.R. and Bray,S.J. (1994) The Drosophila tissue-specific factor Grainyhead contains novel DNA-binding and dimerization domains which are conserved in the human protein CP2. *Mol. Cell Biol.*, **14**, 4020–4031.
68. Bray,S.J., Johnson,W.A., Hirsh,J., Heberlein,U. and Tjian,R. (1988) A cis-acting element and associated binding factor required for CNS expression of the Drosophila melanogaster dopa decarboxylase gene. *EMBO J.*, **7**, 177–188.
69. Liaw,G.J., Rudolph,K.M., Huang,J.D., Dubnicoff,T., Courey,A.J. and Lengyel,J.A. (1995) The torso response element binds GAGA and NTF-1/Elf-1, and regulates tailless by relief of repression. *Genes Dev.*, **9**, 3163–3176.
70. Huang,J.D., Dubnicoff,T., Liaw,G.J., Bai,Y., Valentine,S.A., Shirokawa,J.M., Lengyel,J.A. and Courey,A.J. (1995) Binding sites for transcription factor NTF-1/Elf-1 contribute to the ventral repression of decapentaplegic. *Genes Dev.*, **9**, 3177–3189.
71. Brown,J.L. and Kassis,J.A. (2013) Architectural and functional diversity of polycomb group response elements in Drosophila. *Genetics*, **195**, 407–419.
72. MacFawn,I., Wilson,H., Selth,L.A., Leighton,I., Serebriiskii,I., Bleackley,R.C., Elzamzamy,O., Farris,J., Pifer,P.M., Richer,J. *et al.* (2018) Grainyhead-like-2 confers NK-sensitivity through interactions with epigenetic modifiers. *Mol. Immunol.*, **105**, 137–149.
73. Zhao,Z., Wang,L., Volk,A.G., Birch,N.W., Stoltz,K.L., Bartom,E.T., Marshall,S.A., Rendleman,E.J., Nestler,C.M., Shilati,J. *et al.* (2019) Regulation of MLL/COMPASS stability through its proteolytic cleavage by taspase1 as a possible approach for clinical therapy of leukemia. *Genes Dev.*, **33**, 61–74.
74. Mueller,S., Wahlander,A., Selevsek,N., Otto,C., Ngwa,E.M., Poljak,K., Frey,A.D., Aebi,M. and Gauss,R. (2015) Protein degradation corrects for imbalanced subunit stoichiometry in OST complex assembly. *Mol. Biol. Cell*, **26**, 2596–2608.
75. Tie,F., Banerjee,R., Saiakhova,A.R., Howard,B., Monteith,K.E., Scacheri,P.C., Cosgrove,M.S. and Harte,P.J. (2014) Trithorax monomethylates histone H3K4 and interacts directly with CBP to promote H3K27 acetylation and antagonize Polycomb silencing. *Development*, **141**, 1129–1139.
76. Ardehali,M.B., Mei,A., Zobeck,K.L., Caron,M., Lis,J.T. and Kusch,T. (2011) Drosophila Set1 is the major histone H3 lysine 4 trimethyltransferase with role in transcription. *EMBO J.*, **30**, 2817–2828.
77. Holowatyj,A., Yang,Z.Q. and Pile,L.A. (2015) Histone lysine demethylases in Drosophila melanogaster. *Fly (Austin)*, **9**, 36–44.
78. Curtis,B.J., Zraly,C.B. and Dingwall,A.K. (2013) Drosophila LSD1-CoREST demethylase complex regulates DPP/TGFbeta signaling during wing development. *Genesis*, **51**, 16–31.
79. Whyte,W.A., Bilodeau,S., Orlando,D.A., Hoke,H.A., Frampton,G.M., Foster,C.T., Cowley,S.M. and Young,R.A. (2012) Enhancer decommissioning by LSD1 during embryonic stem cell differentiation. *Nature*, **482**, 221–225.
80. Lee,N., Zhang,J., Klose,R.J., Erdjument-Bromage,H., Tempst,P., Jones,R.S. and Zhang,Y. (2007) The trithorax-group protein Lid is a histone H3 trimethyl-Lys4 demethylase. *Nat. Struct. Mol. Biol.*, **14**, 341–343.
81. Secombe,J., Li,L., Carlos,L. and Eisenman,R.N. (2007) The Trithorax group protein Lid is a trimethyl histone H3K4 demethylase required for dMyc-induced cell growth. *Genes Dev.*, **21**, 537–551.
82. Eissenberg,J.C., Lee,M.G., Schneider,J., Ilvarsonn,A., Shiekhattar,R. and Shilatifard,A. (2007) The trithorax-group gene in Drosophila little imaginal discs encodes a trimethylated histone H3 Lys4 demethylase. *Nat. Struct. Mol. Biol.*, **14**, 344–346.
83. King-Jones,K. and Thummel,C.S. (2005) Nuclear receptors–a perspective from Drosophila. *Nat. Rev. Genet.*, **6**, 311–323.
84. Fay,A., Misulovin,Z., Li,J., Schaaf,C.A., Gause,M., Gilmour,D.S. and Dorsett,D. (2011) Cohesin selectively binds and regulates genes with paused RNA polymerase. *Curr. Biol.*, **21**, 1624–1634.
85. Koenecke,N., Johnston,J., He,Q., Meier,S. and Zeitlinger,J. (2017) Drosophila poised enhancers are generated during tissue patterning with the help of repression. *Genome Res.*, **27**, 64–74.
86. Shao,W. and Zeitlinger,J. (2017) Paused RNA polymerase II inhibits new transcriptional initiation. *Nat. Genet.*, **49**, 1045–1051.
87. Misulovin,Z., Schwartz,Y.B., Li,X.Y., Kahn,T.G., Gause,M., MacArthur,S., Fay,J.C., Eisen,M.B., Pirrotta,V., Biggin,M.D. *et al.* (2008) Association of cohesin and Nipped-B with transcriptionally active regions of the Drosophila melanogaster genome. *Chromosoma*, **117**, 89–102.
88. Gause,M., Webber,H.A., Misulovin,Z., Haller,G., Rollins,R.A., Eissenberg,J.C., Bickel,S.E. and Dorsett,D. (2008) Functional links between Drosophila Nipped-B and cohesin in somatic and meiotic cells. *Chromosoma*, **117**, 51–66.
89. Rao,S.S.P., Huang,S.C., Glenn St Hilaire,B., Engreitz,J.M., Perez,E.M., Kieffer-Kwon,K.R., Sanborn,A.L., Johnstone,S.E., Bascom,G.D., Bochkov,I.D. *et al.* (2017) Cohesin loss eliminates all loop domains. *Cell*, **171**, 305–320.
90. Ing-Simmons,E., Seitan,V.C., Faure,A.J., Flicek,P., Carroll,T., Dekker,J., Fisher,A.G., Lenhard,B. and Merkenschlager,M. (2015) Spatial enhancer clustering and regulation of enhancer-proximal genes by cohesin. *Genome Res.*, **25**, 504–513.
91. Schaaf,C.A., Kwak,H., Koenig,A., Misulovin,Z., Gohara,D.W., Watson,A., Zhou,Y., Lis,J.T. and Dorsett,D. (2013) Genome-wide control of RNA polymerase II activity by cohesin. *PLoS Genet.*, **9**, e1003382.
92. Kvon,E.Z., Kazmar,T., Stampfel,G., Yanez-Cuna,J.O., Pagani,M., Schernhuber,K., Dickson,B.J. and Stark,A. (2014) Genome-scale functional characterization of Drosophila developmental enhancers in vivo. *Nature*, **512**, 91–95.
93. Heinz,S., Romanoski,C.E., Benner,C. and Glass,C.K. (2015) The selection and function of cell type-specific enhancers. *Nat. Rev. Mol. Cell Biol.*, **16**, 144–154.
94. Bernardo,T.J., Dubrovskaya,V.A., Xie,X. and Dubrovsky,E.B. (2014) A view through a chromatin loop: insights into the ecdysone activation of early genes in Drosophila. *Nucleic Acids Res.*, **42**, 10409–10424.
95. Sofueva,S., Yaffe,E., Chan,W.C., Georgopoulou,D., Vietri Rudan,M., Mira-Bontenbal,H., Pollard,S.M., Schroth,G.P., Tanay,A. and Hadjur,S. (2013) Cohesin-mediated interactions organize chromosomal domain architecture. *EMBO J.*, **32**, 3119–3129.
96. Dixon,J.R., Jung,I., Selvaraj,S., Shen,Y., Antosiewicz-Bourget,J.E., Lee,A.Y., Ye,Z., Kim,A., Rajagopal,N., Xie,W. *et al.* (2015) Chromatin architecture reorganization during stem cell differentiation. *Nature*, **518**, 331–336.
97. Sexton,T., Yaffe,E., Kenigsberg,E., Bantignies,F., Leblanc,B., Hoichman,M., Parrinello,H., Tanay,A. and Cavalli,G. (2012) Three-dimensional folding and functional organization principles of the Drosophila genome. *Cell*, **148**, 458–472.
98. Zhou,H.Y., Katsman,Y., Dhaliwal,N.K., Davidson,S., Macpherson,N.N., Sakthidevi,M., Collura,F. and Mitchell,J.A. (2014) A Sox2 distal enhancer cluster regulates embryonic stem cell differentiation potential. *Genes Dev.*, **28**, 2699–2711.
99. Dhar,S.S., Lee,S.H., Kan,P.Y., Voigt,P., Ma,L., Shi,X., Reinberg,D. and Lee,M.G. (2012) Trans-tail regulation of MLL4-catalyzed H3K4 methylation by H4R3 symmetric dimethylation is mediated by a tandem PHD of MLL4. *Genes Dev.*, **26**, 2749–2762.
100. White,K.P., Hurban,P., Watanabe,T. and Hogness,D.S. (1997) Coordination of Drosophila metamorphosis by two ecdysone-induced nuclear receptors. *Science*, **276**, 114–117.
101. Schubiger,M. and Truman,J.W. (2000) The RXR ortholog USP suppresses early metamorphic processes in Drosophila in the absence of ecdysteroids. *Development*, **127**, 1151–1159.
102. Lai,B., Lee,J.E., Jang,Y., Wang,L., Peng,W. and Ge,K. (2017) MLL3/MLL4 are required for CBP/p300 binding on enhancers and super-enhancer formation in brown adipogenesis. *Nucleic Acids Res.*, **45**, 6388–6403.
103. Zhang,Y., Jang,Y., Lee,J.E., Ahn,J., Xu,L., Holden,M.R., Cornett,E.M., Krajewski,K., Klein,B.J., Wang,S.P. *et al.* (2019) Selective binding of the PHD6 finger of MLL4 to histone H4K16ac links MLL4 and MOF. *Nat. Commun.*, **10**, 2314.
104. Rollins,R.A., Morcillo,P. and Dorsett,D. (1999) Nipped-B, a Drosophila homologue of chromosomal adherins, participates in activation by remote enhancers in the cut and Ultrabithorax genes. *Genetics*, **152**, 577–593.

105. Pherson,M., Misulovin,Z., Gause,M. and Dorsett,D. (2019) Cohesin occupancy and composition at enhancers and promoters are linked to DNA replication origin proximity in Drosophila. *Genome Res.*, **29**, 602–612.
106. Zentner,G.E. and Scacheri,P.C. (2012) The chromatin fingerprint of gene enhancer elements. *J. Biol. Chem.*, **287**, 30888–30896.
107. Michieletto,D., Chiang,M., Coli,D., Papantonis,A., Orlandini,E., Cook,P.R. and Marenduzzo,D. (2018) Shaping epigenetic memory via genomic bookmarking. *Nucleic Acids Res.*, **46**, 83–93.
108. Kadauke,S. and Blobel,G.A. (2013) Mitotic bookmarking by transcription factors. *Epigenet. Chromatin*, **6**, 6.
109. Palozola,K.C., Lerner,J. and Zaret,K.S. (2019) A changing paradigm of transcriptional memory propagation through mitosis. *Nat. Rev. Mol. Cell Biol.*, **20**, 55–64.
110. Javasky,E., Shamir,I., Gandhi,S., Egri,S., Sandler,O., Rothbart,S.B., Kaplan,N., Jaffe,J.D., Goren,A. and Simon,I. (2018) Study of mitotic chromatin supports a model of bookmarking by histone modifications and reveals nucleosome deposition patterns. *Genome Res.*, **28**, 1455–1466.
111. Wong,M.M., Byun,J.S., Sacta,M., Jin,Q., Baek,S. and Gardner,K. (2014) Promoter-bound p300 complexes facilitate post-mitotic transmission of transcriptional memory. *PLoS One*, **9**, e99989.
112. Graveley,B.R., Brooks,A.N., Carlson,J.W., Duff,M.O., Landolin,J.M., Yang,L., Artieri,C.G., van Baren,M.J., Boley,N., Booth,B.W. *et al.* (2011) The developmental transcriptome of Drosophila melanogaster. *Nature*, **471**, 473–479.
113. Thummel,C.S. (2001) Molecular mechanisms of developmental timing in C. elegans and Drosophila. *Dev. Cell*, **1**, 453–465.